Soil bacteria override speciation effects on zinc phytotoxicity in zinc-contaminated soils

Soil bacteria override speciation effects on zinc phytotoxicity in zinc-contaminated soils

Nyekachi C. Adele[a*], Bryne T. Ngwenya[a], Kate V. Heal[a], and J. Frederick W. Mosselmans[b]

[a]School of GeoSciences, University of Edinburgh, Edinburgh, UK

[b]Diamond Light Source, Harwell Science and Innovation Campus, Didcot, UK

*Corresponding author contact details:

School of GeoSciences, University of Edinburgh, Grant Institute, James Hutton Road, The King's Buildings, Edinburgh EH9 3FE, UK

Email: kachia6@yahoo.com

TOC

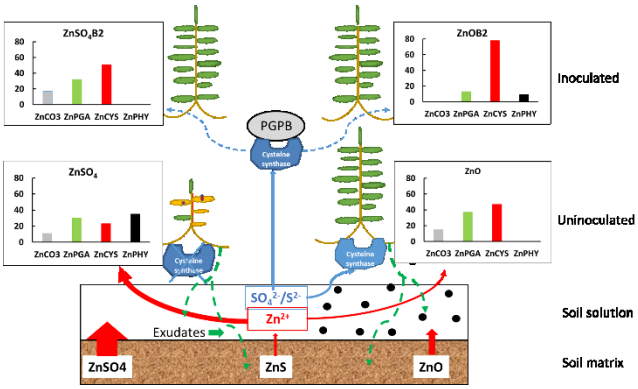

Abstract

The effects of zinc (Zn) speciation on plant growth in Zn-contaminated soil in the presence of bacteria are unknown but are critical to our understanding of metal biodynamics in the rhizosphere where bacteria are abundant. A 6-week pot experiment investigated the effects of two plant growth promoting bacteria (PGPB), *Rhizobium leguminosarum* and *Pseudomonas brassicacearum*, on Zn accumulation and speciation in *Brassica juncea* grown in soil amended with 600 mg kg^{-1} elemental Zn as three Zn species - soluble $ZnSO_4$ and nanoparticles of ZnO

and ZnS. Measures of plant growth were higher across all Zn treatments inoculated with PGPB compared to uninoculated controls but Zn species effects were not significant. Transmission electron microscopy identified dense particles in the epidermis and intracellular spaces in roots, suggesting Zn uptake in both dissolved and particulate forms. X-ray absorption near edge structure (XANES) analysis of roots revealed differences in Zn speciation between treatments. Uninoculated plants exposed to $ZnSO_4$ contained Zn predominantly in the form of Zn phytate (35%), and Zn polygalacturonate (30%), whereas Zn cysteine (57%) and Zn polygalacturonate (37%) dominated in roots exposed to ZnO nanoparticles. Inoculation with PGPB increased (> 50%) the proportion of Zn cysteine under all Zn treatments, suggesting Zn co-ordination with cysteine as the predominant mechanism of Zn toxicity reduction by PGPB. Using this approach we show, for the first time, that although speciation is important, the presence of rhizospheric bacteria completely overrides speciation effects such that most of the Zn in plant tissue exists as complexes other than the original form.

Key words

Speciation, zinc, nanoparticles, plant growth promoting bacteria, phytoextraction, XANES

Introduction

Models of metal uptake by, and toxicity to organisms, including the Free Ion Activity Model (FIAM)[1] and the Biotic Ligand Model (BLM),[2] are rooted in the long established dependence of metal bioavailability on speciation in solution. Development of similarly predictive models for solid phases, such as may exist in soil, has not been possible, in part due to the complexity of solid phase speciation, which involves associations with minerals of differing solubilities and/or redox activities. This has led to a proliferation of operational speciation schemes for estimating potential metal uptake and toxicity. The emergence of nanotechnology has

provided opportunities to advance model development through access to nanoparticles with enhanced solubilities and the potential for direct absorption by organisms. As a result, biotic ligand models are now being tested for their ability to predict metal toxicity from nanoparticulate phases to daphnids and annelids.[3] Preliminary indications are that the biodynamics of nanoparticles depend on the mode of uptake (dissolved versus nanoparticulate) by the organism.

Biotic ligand models have also been used to predict metal uptake by and toxicity to plants, as demonstrated by chloride-enhanced cadmium uptake by *Brassica juncea*.[4] In order to extend this approach to nanoparticles biodynamics, it is necessary to understand how/whether nanoparticles uptake differs from dissolved metal uptake by plants. Although a number of previous studies have shown that speciation is an important factor in determining metal bioavailability and toxicity to plants,[5,6] there is less of a consensus on the mode of metal uptake from nanoparticles. For example, some studies have reported the accumulation of ZnO nanoparticles in plant roots[7,8] whereas others[9-11] did not find ZnO nanoparticles in plants treated with ZnO nanoparticles, suggesting that nanoparticle metal species are transformed into other soluble species after plant uptake.

The aim of this study was to evaluate the role of Zn speciation on its uptake by, and toxicity to *Brassica juncea* grown in soil contaminated with 600 mg kg^{-1} equivalent Zn. Zinc was chosen because it is a widespread metallic soil contaminant with anthropogenic sources including mine tailings, smelter slags, and fertilizers.[12] Following release, Zn predominantly occurs in soil as sphalerite (ZnS) and zincite (ZnO).[13] These two forms of Zn are also widely used in engineered nanomaterials within gas sensors, ultraviolet detectors, photovoltaic devices and personal care products,[14,15] leading to potential release in the environment, which may alter the soil-plant system.[16-18] Although Zn is vital for plant health, with up to 30%

of cultivated soils globally having low phytoavailable Zn, resulting in Zn deficiency in soils and plants,[19] excess Zn can be detrimental, inducing physiological, morphological and biochemical dysfunctions in plants such as impaired plant growth, reduced chlorophyll and seed production, and development of chlorosis and necrosis.[20,21] *Brassica juncea* (L.) Czern. was chosen for this study as a known Zn hyperaccumulator[22-24] which nevertheless is sensitive to Zn at high concentrations, and is thus suitable for investigating the bioavailability and toxicity of Zn species present in soil.[23] Besides primary Zn speciation, we also investigated the role of rhizospheric bacteria. Rhizosphere-associated microorganisms are naturally occurring microbes growing in association with plant roots and are known to change metal speciation, increase metal solubility, and act additively on plant health,[25-27] through secretion of phytohormones,[28] production of chelators,[29] acidification and biomineralization.[30]

The objectives of this study were to: (i) assess the role of Zn speciation on growth of *Brassica juncea*; (ii) investigate the role of rhizospheric bacteria on growth of *B. juncea* exposed to different Zn species; (iii) compare Zn uptake and accumulation between inoculated and uninoculated plants; and (iv) evaluate Zn speciation in inoculated and uninoculated roots of *B. juncea* exposed to different Zn species.

2 Materials and Methods

2.1 Selection of materials and preliminary materials characterization

Brassica juncea (L.) Czern was chosen for this study as a demonstrated excellent hyperaccumulating plant known to tolerate and accumulate high amounts of metal in their

95 living aboveground biomass.[22-24] Seeds were purchased from Sow Seeds Ltd., UK, and stored
96 in a plastic bag in the dark at temperature 14 -16°C until use.

97 Zinc sulfate and ZnO nanoparticles (particle size <35 nm) were purchased from Sigma
98 Aldrich, UK, and stored according to vendor instructions, while ZnS nanoparticles were
99 synthesized in our laboratory using a chemical precipitation method.[31] ZnS nanoparticles
100 were made from 1 M aqueous solutions of Na_2S and $ZnCl_2$. The morphology of ZnO
101 nanoparticles and ZnS nanoparticles were characterized using transmission electron
102 microscopy (TEM, Philips CM120 instrument), while ZnS nanoparticles structure was
103 determined by X-ray diffraction (XRD, Bruker D2 PHASER diffractometer). For the latter, 0.1 g
104 of dry powdered ZnS sample was measured on a Bruker D2 PHASER diffractometer fitted with
105 a LynxEye detector and operating in a flat plate mode using Ni-filtered Cu K-alpha radiation
106 (λ= 1.54060 Å) (start: 5°; end: 90°; time per step: 0.3 s). The crystallite size was calculated
107 from the Debye-Scherrer formula (Eq. 1),[32]

108 $$D = \frac{K\lambda}{\beta cos\theta} \qquad (Eq. 1)$$

109 where D is the mean diameter of the crystallite (nm), k is a constant related to the
110 dimensionless shape (0.94), λ is the X-ray wavelength (Å), β is the full width at half the
111 maximum intensity (radians, r) and θ is the corresponding diffraction angle (°).

112 Further characterization of ZnO and ZnS nanoparticles involved conducting a 4-day
113 dissolution experiment in ultrapure water starting with a nominal concentration of 600 mg L^{-1}
114 elemental Zn, consistent with the Zn dose in the experimental soil (details in Supporting
115 Information S5). Microcosms were set up in duplicate, and sampled once per day using a
116 syringe followed by centrifugal filtration through a 3 kD pore filter for 30 min at 5,000 x g. The

117 filtrate was acidified to 2% in HNO_3 acid and analyzed for dissolved Zn using ICP-OES alongside
118 a certified ICP multi-element standard solution VI (Merck).
119 Soil amended with peat has been reported to influence metal speciation by modifying
120 metal mobility and availability due to a high organic matter content.[33] Organic matter can also
121 influence sulfur speciation and, since ZnS was one of the Zn forms used in the study, soils
122 containing peat were avoided. Instead, unamended topsoil (Westland topsoil, Dobbies
123 Garden Centre, Edinburgh, UK) was used to represent an environmentally relevant soil
124 containing all the nutrients required for plant growth. Measured soil physicochemical
125 properties are reported in Supporting Information S1.
126
127 **2.2 Pot experiments**
128 Pot experiments were conducted using sterilized (134^{o}C for 4 min in a BMM Weston
129 autoclave) air-dried soil contaminated with 600 mg Zn kg^{-1} of $ZnSO_4$, ZnS and ZnO
130 nanoparticles. The Zn concentration chosen was 600 mg Zn kg^{-1} which was sufficient to trigger
131 toxic effects in plants[34,35] without completely curtailing growth. For the nanoparticles, an
132 appropriate amount of nanoparticles required to spike 9 kg of soil with equivalent 600 mg kg^{-1}
133 elemental Zn was dissolved in ultrapure water and dispersed by sonication (Decon Fs 200b
134 sonicator, 30^{o}C) for 1 hr using the procedure of Lin and Xing.[7] Following sonication, the
135 suspension was transferred to the soil and mixed by hand for 1 h to produce a homogeneously
136 mixed soil. Each 2.15 L pot contained 1 kg of spiked ($ZnSO_4$, ZnO and ZnS) or un-spiked soil
137 (control) and equilibrated for 1 week before planting (see Supporting Information S2).
138 Inoculation was conducted through treatment of *Brassica juncea* seeds as follows. Seeds were
139 surface sterilized with 5% NaClO for 15 min and washed three times with sterile deionized
140 water. Seeds were soaked for 4 h in 10 mL bacteria suspension (*Rhizobium leguminosarum*

bv. *trifolii* or *Pseudomonas brassicacearum)* and uninoculated seeds were soaked in sterilized deionized water over the same duration before sowing five seeds in each pot (Supporting Information S2). The experiments were conducted in a greenhouse at the School of Biological Sciences, University of Edinburgh, with mean 21°C daytime and 18°C night-time temperatures, and artificial lighting providing a photoperiod of 18 h d^{-1} and photo levels of ~150 µmol m^{-2} s^{-1}. Although the greenhouse is a non-sterile environment, we reasoned that environmental microbes within the greenhouse will colonize all treatments equally so initial sterilization of the soil simply provided a baseline reference point. Pot experiments (Supporting Information S2) contained 12 triplicate treatments (including controls), in which *Brassica juncea* were grown with and without the presence of bacteria and were distributed randomly in the greenhouse. All plants were harvested 6 weeks after planting of seeds.

2.3 Plant sampling and bioaccumulation analysis

Metal-related phytotoxicity was evaluated by measuring weekly plant height, dry biomass at the end of the experiment (6 weeks after seed planting), and through other observations such as leaf chlorosis and necrosis. Total Zn concentrations in duplicate sub-samples of the ground plant materials and soil (batched for each treatment from the 3 replicate pots) were determined as described by Allen et al.[36] (6 mL concentrated HCl and 1 mL HNO_3 were used for digestion of 0.5 g ashed soil samples and 2 mL concentrated H_2SO_4 and 0.75 mL H_2O_2 (30%) for digestion of 0.1 g plant material samples). Zn concentrations in the digests were determined by inductively coupled plasma-optical emission spectrometry (ICP-OES) (Perkin Elmer Optima 5300DV). Zn contents were expressed as mg kg^{-1} (dry weight) as single values for each treatment and used to evaluate Zn uptake by the plant, by calculating

bioaccumulation factors (BCF), translocation factors (TF) and phytoextraction efficiency (PE) as detailed in Supporting Information S3.

2.4 Synchrotron based X-ray spectroscopic (XAS) analysis

Using fresh plants grown in the same way, μXRF (micro X-ray fluorescence) and μXAS measurements of roots and shoots of *B. juncea* were studied in a liquid nitrogen cryostat on beamline I18 at Diamond Light Source, Oxford, United Kingdom[37] (details in Supporting Information S4). The XRF maps were analysed in PyMCA 4.4.1 software.[38] MicroXANES Zn K-edge data were compared to spectra from a range of standards[23] using the program ATHENA.[39] Zn standards comprised ZnS nanoparticles, Zn oxalate, Zn phosphate, Zn histidine, Zn cysteine, Zn phytate, Zn formate, Zn polygalacturonate and ZnO nanoparticles.

2.5 Data analysis

The means and standard error (SE) of plant height, dry shoot and root biomass and metal concentrations in soil and plant samples were calculated for each treatment. Statistical analyses were conducted using Minitab software version 17 (Minitab TM Inc., State College, PA, USA), with significance level $p<0.05$. All treatment means were found to be normally distributed using Anderson-Darling's test. General Linear Models (GLM), followed by Tukey's HSD tests were used to identify any significant differences between treatments. The GLMs contained fixed factors of Zn species (four levels – uncontaminated control and the three different Zn species) and bacteria inoculation (three levels – uninoculated control and the two different PGPB) and the interaction of the two factors.

3. Results and Discussion

3.1 Phase characterization of ZnS nanoparticles

XRD analysis of the synthesized ZnS nanoparticles in (Supporting Information S5) showed three broad peaks at 2Θ angle of 28.5, 48.2 and 56.5 corresponding to lattice planes of (111), (220) and (311) in the structure of ZnS sphalerite, respectively. This is consistent with the crystal structure of the standard code (ICSD No. 01-0729269) for ZnS. The crystallite size was 86.5 Å (8.65 nm) as calculated from the Debye-Scherrer formula. TEM images of the synthesized ZnS nanoparticles in (Supporting Information S5) indicate that the material occurred in clusters.

3.2 Growth parameters under different Zn species and bacterial treatments

Figure 1 shows *B. juncea* plant height, shoot dry biomass and root dry biomass at 6 weeks of growth for all Zn species and bacteria inoculation treatments and controls. GLM analyses of these growth parameters showed significant effects of the individual factors, Zn species and bacteria inoculation. Tukey HSD tests revealed significant differences in shoot and dry root biomass due to the interaction of the Zn species and bacteria inoculation factors represented by different letters in Figures 1B-C but not for plant height (Figure 1A). Shoot dry biomass (Figure 1B) was significantly lower in the Zn treatments compared to the control with no added Zn across all bacterial inoculation treatments. However, there was no significant difference in shoot dry biomass between the uninoculated control and inoculated $ZnSO_4$ treatments, suggesting that the presence of PGPB offset the effect of $ZnSO_4$ contamination on shoot dry biomass. Root dry biomass in the uninoculated treatments (blue bars in Figure 1C) was not significantly different between the uncontaminated control and the different Zn species, apart from for the $ZnSO_4$ treatment which had significantly lower root dry biomass.

209 Similarly to shoot dry biomass, there appeared to be a restorative effect of PGPB on root dry
210 biomass for the $ZnSO_4$ treatments as there was no significant difference in root dry biomass
211 between the inoculated $ZnSO_4$ treatments and the uninoculated control. Shoot and root dry
212 biomass were significantly lower in the Zn treatments compared to the control with no added
213 Zn, whilst plant height and shoot and root dry biomass were significantly higher in the
214 inoculated compared to the uninoculated treatments.

215 Plant height was significantly lower in soil amended with ZnO nanoparticles across all
216 bacteria inoculation treatments, compared to the no added Zn and $ZnSO_4$ and ZnS
217 nanoparticles treatments (Tukey HSD tests on Zn species factor, not shown in Figure 1A).
218 However, from visual observation during the experiment, the uninoculated $ZnSO_4$ treatment
219 appeared to be the most phytotoxic as the *B. juncea* (L.) Czern. plants showed visible
220 symptoms of toxicity (yellowing of leaves). These symptoms became more severe with
221 increasing exposure time as the leaves of the plants began to wilt and fall off after 6 weeks of
222 growth. There were no symptoms of toxicity in plants grown in soil amended with ZnS and
223 ZnO nanoparticles throughout the experiment. In the absence of inoculation with PGPBs,
224 addition of any of the Zn species investigated had a detrimental effect on shoot dry biomass,
225 although differences amongst Zn species were not statistically significant.

226 Hence plants exposed to $ZnSO_4$ were more adversely affected, followed by those
227 exposed to ZnO and then ZnS, although growth differences were not statistically significant.
228 Previous studies have shown that soluble Zn is more toxic to plant growth compared to other
229 forms of Zn.[40, 41] We hypothesized that these differences reflect the relative solubilities of the
230 Zn species applied, since solubility of these species increases in the order $ZnS<ZnO<<ZnSO_4$.[40]
231 Indeed, studies have shown that when applied to soils, ZnO dissolves much faster than ZnS
232 (e.g. [42]). Our nanoparticle dissolution experiments did not confirm this trend, with

concentration of Zn being slightly lower in ZnO suspensions (Supporting Information Figure S2), although the differences are small (~0.4 mg L^{-1}). During the experiment, we noted significant aggregation of the ZnO nanoparticles (Supporting Information Figure S3), a feature also reported by numerous previous studies.[43, 44] Thus, all else being equal, it is likely that Zn concentrations in ZnO will be higher in our soil systems. We have confidence in our measured concentrations based on comparison with previous studies for ZnO (e.g. [44]) for similar nominal nanoparticle sizes, but our measured concentrations are much higher than those measured for ZnS,[45] potentially due to different synthesis routes.

Zinc is a micronutrient required for plant health, playing an important role in plant metabolism by influencing the activities of hydrogenase and carbonic anhydrase, as well as in the synthesis of tryptophan, a precursor to indoleacetic acid synthesis.[46] Consequently, Zn stimulates *B. juncea* growth at low concentration[47, 48] but at higher concentration causes significant suppression of plant growth. We did not observe any growth promotion effect (relative to controls without Zn addition) even in the presence of nanoparticles, suggesting that nanoparticles supply enough dissolved Zn to exceed the beneficial threshold. Negative effects of ZnO nanoparticles on plant growth and biomass have been reported by other workers.[7,49] The current study is the first, to the best of our knowledge, to investigate plant response to ZnS nanoparticle-contaminated soil. Our results suggest that ZnS nanoparticles are less phytotoxic compared to ZnO nanoparticles and $ZnSO_4$ as indicated by plant height and visible symptoms of phytotoxicity.

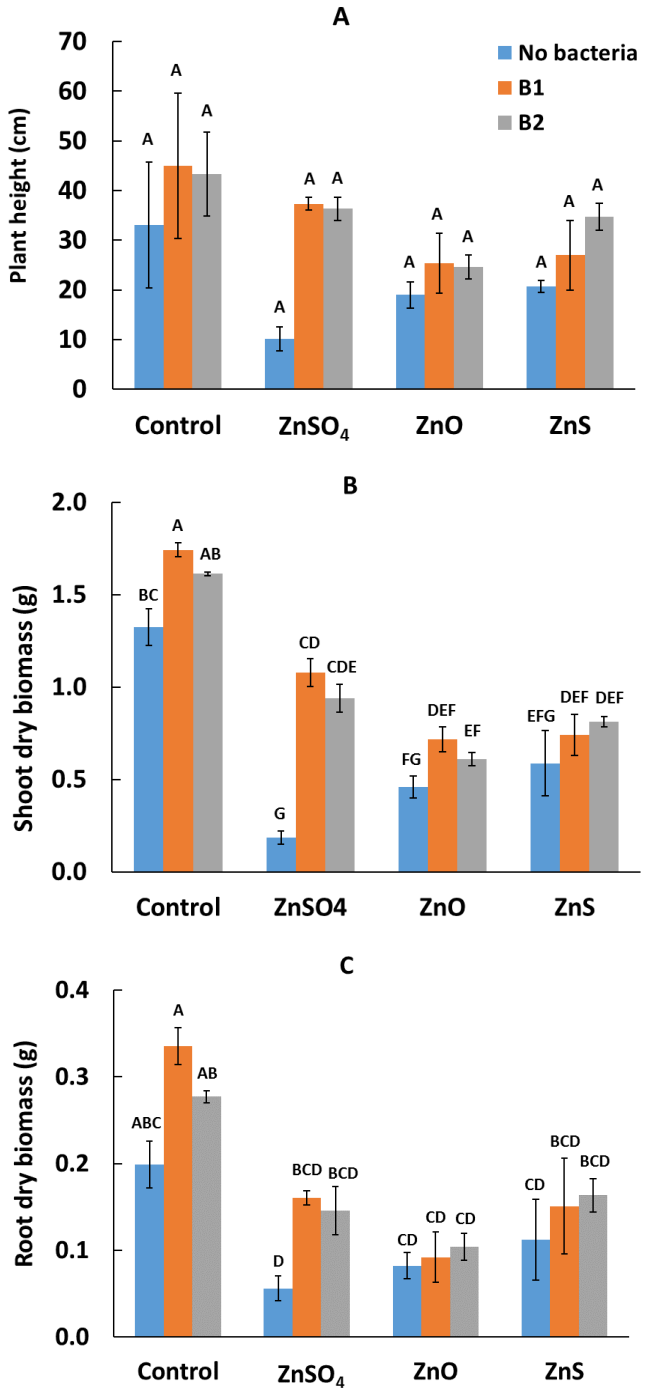

Figure 1. Plant height (A), shoot dry biomass (B) and root dry biomass (C) of *B. juncea* after 6 weeks growth in unamended and contaminated soil to which 600 mg kg^{-1} elemental Zn was applied in the form of $ZnSO_4$ and ZnO and ZnS NPs, comparing inoculated and uninoculated treatments. B1 represents *R. leguminosarum* and B2 is *P. brassicacearum*. Bars are means ± standard error of three pots. In (B) and (C) different capital letters above the bars indicate significant differences in biomass between treatments ($p<0.05$, determined by GLM followed by Tukey HSD tests). In (A) the capital letters above the bars are identical, indicating no significant differences in plant height between treatments.

In contrast to speciation effects, our study showed significant increases in plant height and dry shoot and root biomass across all Zn species treatments when seeds were inoculated with bacteria (Tukey HSD tests on bacteria inoculation factor, not shown in Figure 1). Mean plant height and shoot and root biomass were higher in the Zn treatments inoculated with bacteria, compared to the uninoculated treatments, suggesting greater tolerance of plants to Zn stress from contaminated soils upon inoculation with bacteria. However, the increase was significant only for shoot biomass for the $ZnSO_4$ treatment (Figure 1B), where it could also be explained as a sulfur-promoted increase in growth.[50-51] The potential for *R. leguminosarum* and *P. brassicacearum* to enhance growth in inoculated *B. juncea* plants may be attributed to reported PGPB properties beneficial for plant growth,[27,52] including solubilization of phosphate and the production of indole acetic acid (IAA), ACC deaminase, and siderophores.[53-55] However, these PGPB properties were not examined in this study.

3.3 Effects of Zn speciation and bacteria on Zn uptake and translocation

Shoot concentrations of Zn followed the trend $ZnSO_4$>ZnO>ZnS (Supporting Information Figure S4A) across all treatments, consistent with the growth suppression described above. Within each Zn species treatment, shoot concentrations increased upon inoculation with bacteria, except for ZnO treatments where bacteria appear to have no effect. By contrast, Zn concentrations in roots did not respond to bacterial inoculation except in ZnO treatments, whilst root concentrations also followed the trend $ZnSO_4$>ZnO>ZnS for uninoculated treatments (Supporting Information Figure S4B). Consequently, BCFs (Table 1) calculated from the biomass and soil concentration data were all > 1 except for ZnS nanoparticles treatments with no bacteria and with *P. brassicacearum* (B2) inoculation.

Table 1. Bioaccumulation factors, translocation factors and phytoextraction efficiency in *Brassica juncea* after 6 weeks of growth in soils amended with 600 mg Zn kg^{-1} of different Zn species with and without inoculation with PGPB. B1 represents *R. leguminosarum* and B2 represents *P. brassicacearum*.

Parameter	**Treatment**								
	$ZnSO_4$			**ZnO nanoparticles**			**ZnS nanoparticles**		
	No bacteria	**B1**	**B2**	**No bacteria**	**B1**	**B2**	**No bacteria**	**B1**	**B2**
Bioaccumulation factor (BCF)	1.78	1.85	2.00	1.19	1.39	1.45	0.27	1.15	0.46
Translocation factor (TF)	2.18	2.25	2.38	3.01	1.99	1.77	2.43	1.33	5.54
Phytoextraction efficency (PE, %)	0.05	0.28	0.26	0.04	0.07	0.06	0.01	0.04	0.03

Values of BCF were higher in the inoculated than uninoculated treatments for all Zn species. TF values were > 1 in the inoculated and uninoculated treatments for all Zn species but, when plants were inoculated, TF varied between the different Zn species treatments. TF values increased slightly in inoculated plants growing in $ZnSO_4$ contaminated soils, compared to uninoculated plants. The opposite response occurred in ZnO nanoparticles contaminated soils, with lower TF values occurring in the inoculated compared to the uninoculated plants. In the ZnS contaminated soils, compared to uninoculated plants, the TF value also decreased in plants inoculated with *R. leguminosarum* (B1) but increased in plants inoculated with *P. brassicacearum* (B2). Zn mass removal by *B. juncea* was estimated to compare the phytoextraction efficiency (PE) of Zn by inoculated and uninoculated plants from soil contaminated with different Zn species after 6 weeks of plant growth. Measurable changes in phytoextraction efficiencies were only associated with $ZnSO_4$ treatments, increasing by

about an order of magnitude upon bacterial inoculation, with no differences between the two bacteria (Table 1).

Plants are considered as potential species for phytoextraction if both BCF and TF are > 1.[56] In this study, BCF and TF values varied with different Zn species. BCF was > 1 for inoculated and uninoculated $ZnSO_4$ and ZnO treatments, but was < 1 for uninoculated ZnS and ZnS treatments inoculated with *R. leguminosarum* and ~1 for ZnS treatments inoculated with *R. leguminosarum*. TF values were > 1 for all inoculated and uninoculated Zn treatments, indicating effective translocation of Zn from roots to shoots. Our results are consistent with previous studies showing *B. juncea* to be a Zn hyperaccumulator.[57-58] However, the overall phytoremediation potential was extremely low, with a maximum of 0.28% Zn mass from the soil extracted by plants over 6 weeks in the $ZnSO_4$ treatments in the presence of bacteria (Table 1). Our findings are similar to other studies that have reported that inoculation with PGPB increases plant growth, metal uptake, tolerance and phytoremediation in contaminated soils.[59-60] In contrast, another study reported that PGPB inoculation increased plant growth and Ni tolerance but reduced Ni uptake in plants.[61] This suggests that different PGPBs elicit different responses that may also depend on the hyperaccumulator species.[54-55]

3.4 Distribution of Zn in *Brassica juncea* root biomass

Due to similar growth of plants inoculated with the two different strains of PGPB, only plants inoculated with *P. brassicacearum* were selected for transmission electron microscopy (TEM) (Figure 2). TEM micrographs indicated differences in the morphology and location of Zn in roots of *B. juncea* depending on Zn species. In the Zn nanoparticles treatments, roughly spherical Zn nanoparticles were observed, for example on the epidermis and root surfaces in the ZnO nanoparticles treatment (Figure 2B). In the roots of inoculated plants, less bacteria

346 were evident in the nanoparticles treatments (Figure 2E-F) compared to the $ZnSO_4$ treatment,

347 where they occurred around the root epidermis (Figure 2D).

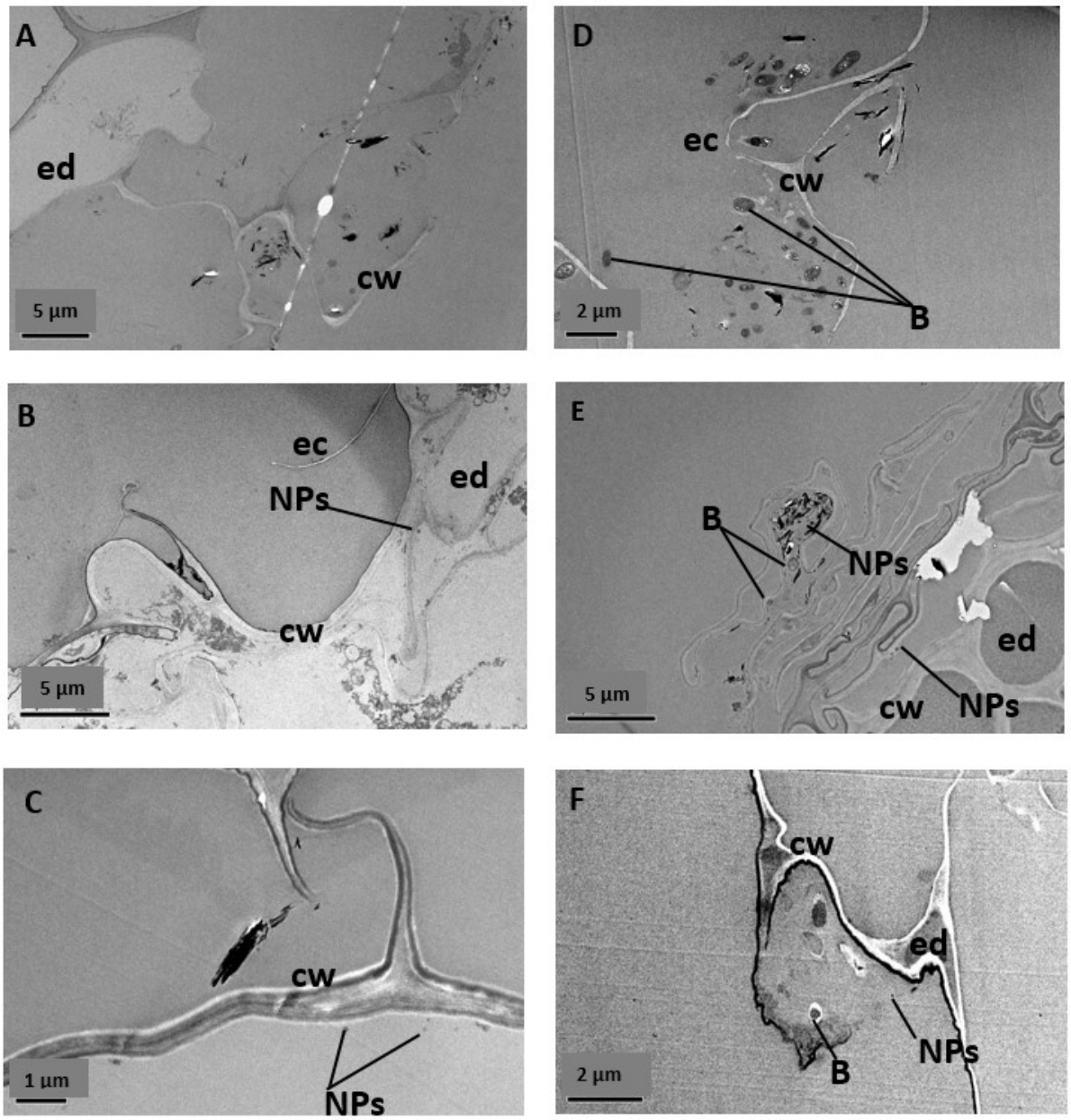

348

349 **Figure 2.** TEM micrograph of a root cross section (bar 1-5 µm) of (A-C) uninoculated $ZnSO_4$,
350 ZnO nanoparticles and ZnS nanoparticles and (D-F) inoculated roots exposed to 600 mg kg^{-1}
351 $ZnSO_4$, ZnO nanoparticles and ZnS nanoparticles, after 6 weeks of growth. Labels in the root
352 cell indicate: NPs - nanoparticles, cw - cell wall, ed - endodermis, ec - epidermis cell, B -
353 *Pseudomonas brassicacearum.*

354

355

Micro-XRF intensity maps showing relative spatial distribution of Zn concentrations are shown in Figure 3, where uninoculated roots are compared with those inoculated with *P. brassicacearum*. The distribution of Zn varied with Zn species. The highest Zn concentrations were in roots treated with ZnO (Figure 3B, E), where the cortex exhibited Zn concentrations that were about an order of magnitude higher than the epidermis.

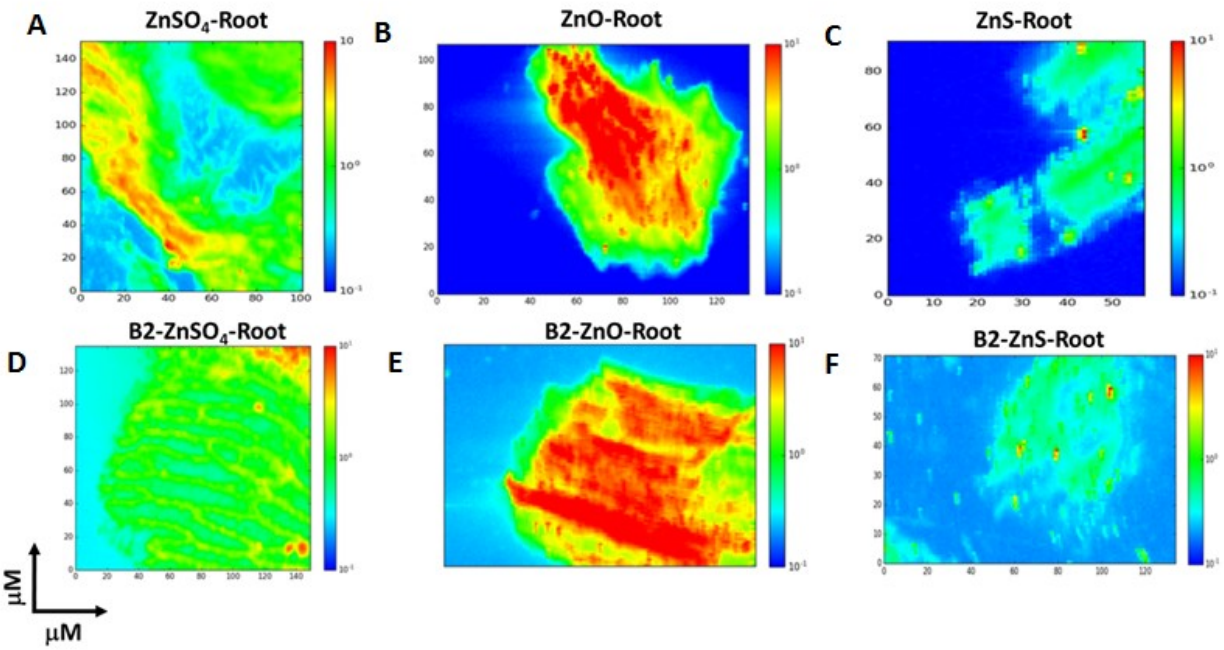

Figure 3. Synchrotron µXRF maps of the transverse section of fresh roots from (A-C) uninoculated and (D-F) inoculated (*P. brassicacearum*) *B. juncea* plants grown in soil treated with 600 mg Zn kg^{-1} of $ZnSO_4$, ZnO and ZnS nanoparticles. Pixel brightness is displayed in RGB; red represents relatively higher Zn intensity, and blue low Zn signal. Fluorescence counts for each map have been normalized to background and the normalized counts plotted on the same scale for visual comparison.

In $ZnSO_4$ treatments, localized Zn hotspots were evident, but the most distinctive characteristic was that high Zn concentrations occurred in the form of stripes (Figure 3A, D). Single hotspots of high Zn concentration were also evident. ZnS treatments showed the lowest Zn concentrations levels with high Zn concentrations occurring as single hotspots (Figure 3C, F). Hotspots of Zn in the roots treated with ZnO and ZnS nanoparticles may indicate the presence of Zn nanoparticles. Comparison between inoculated (Figure 3D-F), and

uninoculated (Figure 3A-C) plants showed no significant impact of bacteria inoculation on Zn concentrations in the root in each treatment. This is entirely consistent with whole root analysis data (Supporting Information Figure S4B).

The observed spatial distribution of Zn in the roots of *B. juncea* suggests that uptake of Zn by *B. juncea* is dependent on the form of Zn contamination in soil, with Zn hotspots observed in roots of plants grown in nanoparticles treatments. Whilst both imaging techniques pointed to the presence of nanoparticulate forms in roots exposed to ZnO and ZnS, nanoparticulate uptake could not be unambiguously confirmed because we did not have analytical capability on the TEM to check the composition. Nevertheless, other studies have reported that cellular penetration by nanoparticles is the mode of action by which nanoparticles interact with plants.[26] Once inside a plant cell, nanoparticles can be transported apoplastically or symplastically through plasmodesmata.[26, 62]

3.6 Speciation of Zn in *Brassica juncea* plants by XANES

Zn μXANES spectra were acquired on some of the Zn hotspots identified by μXRF mapping to determine Zn speciation using linear combination fitting (LCF) of spectra from selected Zn standards. The best fits, based on residual R factors, are presented in Supporting Information S7 for $ZnSO_4$ and ZnO treatments only (data for ZnS treatments was not considered to be of good enough quality). The percentages of species contributing to the LCF are presented in Figure 4.

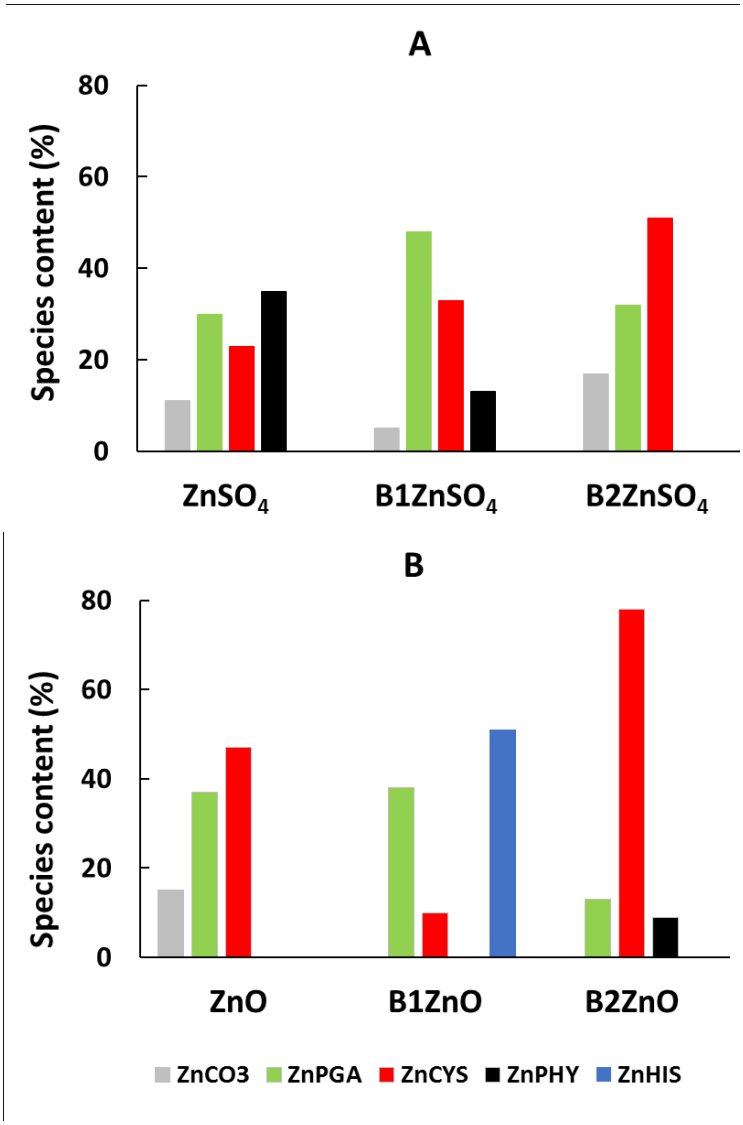

Figure 4. Linear combination fitting of (a) $ZnSO_4$ and (b) ZnO data from hotspots of Zn µ-XRF mapping in *Brassica juncea* roots. Data presented are for individual samples/treatments. Bar charts represent contribution (%) of the various species to the spectra of treatments uninoculated and inoculated with *Rhizobium leguminosarum* (B1) and P*. brassicacearum* (B2). Zn standards are $ZnCO_3$ - Zn carbonate, ZnPHY - Zn phytate, ZnHIS - Zn histidine, ZnCYS- Zn cysteine and ZnPGA - Zn polygalacturonate.

Most samples required 4 components to fully fit the data. Roots grown in $ZnSO_4$ contaminated soil showed that Zn was in the form of Zn phytate (35%), Zn polygalacturonate (30%), Zn cysteine (23%) and Zn carbonate (11%) in uninoculated plants. Roots inoculated with *R. leguminosarum* (B1) showed predominance of Zn polygalacturonate (48%) followed by Zn cysteine (33%) with subordinate amounts of Zn phytate (13%) and Zn carbonate (5%),

while those inoculated with *P. brassicacearum* (B2) showed predominance of Zn cysteine predominating (51%), followed by Zn polygalacturonate (32%) and Zn carbonate (17%) but there was no Zn phytate. In all cases, the inclusion of Zn sulfate did not improve fits to the data. For the ZnO nanoparticles-contaminated soil without bacteria inoculation, fitting showed Zn cysteine (57%) to be the dominant Zn form, followed by Zn polygalacturonate (37%) and Zn carbonate (15%). Roots inoculated with *R. leguminosarum* required Zn histidine (51%) to fully fit the data, being the only plants showing this species, accompanied by Zn polygalacturonate (38%) and Zn cysteine (10%). Finally, roots inoculated with *P. brassicacearum* showed the dominant form of Zn to be Zn cysteine (78%), with minor amounts of Zn polygalacturonate (13%) and Zn phytate (9%).

Thus, our analysis displays common species associated with Zn exposure to plants. Zn phytate (inositol hexakis phosphate), $C_6H_{18}O_{24}P_6$; IP6) is a complex phosphate-containing molecule with a negatively charged phosphate group that forms stable complexes with ions including Zn^{2+}.[8, 63] The presence of Zn phytate in roots has been suggested as a Zn tolerance mechanism in non-hyperaccumulating plants,[64-65] and recently Zn phytate was identified in *B. juncea* to contribute to Zn tolerance,[66] in addition to Zn carbonate complexes. The presence of Zn polygalacturonate is also consistent with previous studies showing that cell wall associated Zn is bound to polygalacturonate.[67] Complexation of Zn with carboxylic acids such as PGA (the main component of pectin in the cell wall) has been reported as a response mechanism to metal toxicity in plants exposed to high Zn concentrations.[63,66]

In effect, inoculation with bacteria is associated with a switch from phytate-polygalacturonate dominated Zn speciation to cysteine-polygalacturonate dominated speciation in roots of plants challenged with $ZnSO_4$. This switch is consistent with previous studies in our laboratory, where significant Zn cysteine speciation only occurred in bacteria-inoculated roots.[23,66] Unlike those studies, however, we also found significant Zn cysteine speciation in uninoculated roots in this study for $ZnSO_4$ treatments. These differences may depend on the plant species and experimental conditions. Cysteine synthesis is widely recognized as a natural response by plants to toxic metal exposure.[68] Our findings suggests that the cysteine synthesis machinery was not completely disabled in these plants, perhaps due to differences in the type of soil used in the two studies.

Nanoparticles treatments, represented by ZnO, exhibit some notable differences from $ZnSO_4$ treatments. Firstly, Zn cysteine complexes represent a significant proportion of the overall speciation in uninoculated treatments, which may be further evidence that the lower solubility of ZnO does not compromise the cysteine synthesis machinery. The high proportion of cysteine complexation in roots exposed to ZnO nanoparticles was unexpected as sulfur was not supplied, but can be explained by the presence of 248.7 mg S kg^{-1} in the soil (Supporting Information S1). Secondly, Zn histidine complexation dominates Zn speciation in roots inoculated with *R. leguminosarum*, and this appears to occur at the expense of Zn cysteine complexation (note that Zn cysteine still dominates in roots inoculated with *P. brassicacearum*). Zn histidine has been reported in previous studies, and is thought to help reduce the toxicity of Zn to the plant,[8,41,65] being a ligand for binding metals in hyperaccumulator species,[69] including Zn.[70] Adediran et al.[71] also reported Zn histidine complexation in roots of *Vicia sativa*, and this was thought to be controlled by nitrogen

metabolism potentially driven by legume-associated symbiotic bacteria. This may explain why we also see it only in plant roots inoculated with *R. leguminosarum*.

Finally, LCF showed a complete absence of ZnO nanoparticles in roots of *B. juncea,* despite TEM suggesting internalized nanoparticles, likely due to these making up a smaller fraction of total Zn. It also suggests that nanoparticulate phases may have to be dissolved before Zn can be taken up by plants.[10] As such, our observations are consistent with some recent studies reporting the absence of nanoparticulate ZnO in plants exposed to ZnO nanoparticles, where Zn was in the form of nitrates, citrate and phosphates.[9-10] However, other studies have reported internalization of ZnO nanoparticles in different plants.[72] It appears that whether nanoparticles are taken up by plants depends on the nanoparticle composition, the growth medium and the plant species involved.[16, 73]

3.7 Environmental implications

Speciation is an important parameter determining metal bioavailability and, in solution at least, has formed the basis of the Free Ion Activity Model for predicting metal bioavailability to cells.[1] This study evaluated the effect of three different Zn species on plant growth, Zn phytotoxicity, Zn accumulation and Zn distribution in roots of a hyperaccumulator species (*B. juncea* (L.) Czern.), known for its Zn hyperaccumulative properties.[59] In addition, we investigated whether inoculation with bacteria modified Zn speciation in plants. Based on our observations, we suggest a mechanistic model of the role of PGPB in ameliorating Zn phytotoxicity through changes in Zn speciation (Figure 5), focusing on root and rhizospheric processes. Although we do not have speciation data for ZnS treatments, we include it in the general model due to similarities in plant growth data to ZnO treatments.

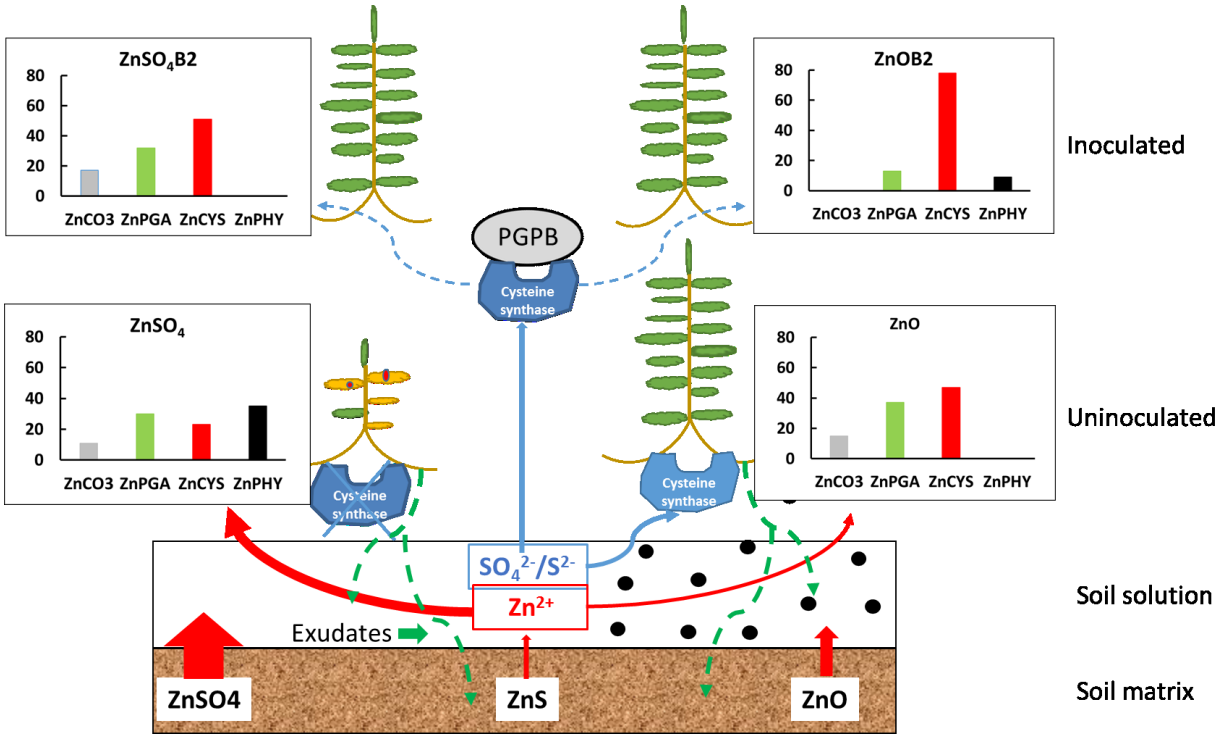

Figure 5. Conceptual model of zinc biodynamics as revealed from plant growth experiments in which the form of 600 mg kg^{-1} Zn applied to soil in which *B. juncea* was grown for 6 weeks was varied, using inoculation data for *P. brassicacearum* only. Explanation of the arrows is provided in the text.

The model emphasizes the inference that Zn is mostly taken up as Zn^{2+}, in part facilitated by production of plant root exudates (green dashed arrows), with cysteine synthesis (red bars) as the main mechanism of Zn detoxification (ignoring Zn histidine in *R. leguminosarum* inoculations). When exposed to high concentrations of soluble $ZnSO_4$, in the uninoculated treatment cysteine synthesis may be disabled (shown by blue cross through "cysteine synthase"), leading to enhanced metal toxicity. This inference is based on the observation of lower Zn cysteine in roots in the uninoculated $ZnSO_4$ treatment, despite this treatment supplying the most sulfate for plant/bacterial metabolism, and also takes into account previous growth experiments in compost where Zn cysteine was not detected.[19] However,

514 this hypothesis remains to be tested by detailed molecular level studies of the biochemistry
515 of the response of *B. juncea* upon exposure to varying Zn^{2+} concentrations. Nevertheless,
516 circumstantial evidence for this inference is that when inoculated with bacteria, roots
517 exposed to $ZnSO_4$ synthesize more cysteine, and plants grow as well as those exposed to
518 nanoparticulate Zn and/ or controls without Zn addition.

519 The model shares some attributes with that published by Adediran et al.,[66] which was
520 based purely on $ZnSO_4$ contamination, but there are important differences that arise from
521 varying the speciation of Zn supplied to soil. The new model includes the role of solubility in
522 controlling Zn bioavailability to plant roots, with higher dissolved Zn^{2+} from $ZnSO_4$, denoted
523 by larger red arrows, being the main determinant of toxicity, particularly when plants were
524 not inoculated with bacteria. This is entirely consistent with existing models of metal
525 bioavailability and phytotoxicity.[60-62]

526 Paradoxically, Zn cysteine was detected in roots exposed to ZnO nanoparticles where
527 no sulfur is supplied to the soil. However, analysis of the soil showed that it contained a
528 significant amount of sulfur (248.7 mg kg^{-1}), so this result is entirely consistent with the model
529 of cysteine synthesis through sulfur metabolism. Lastly, the model captures the observation
530 that, in addition to soluble Zn^{2+}, TEM revealed that Zn was also taken up in nanoparticulate
531 form albeit at much lower quantities (11%). It remains to be established whether PGPB-driven
532 changes in Zn speciation occur in plant roots or at the soil- rhizosphere-plant interface. Finally,
533 we acknowledge that our findings are limited to the single concentration used in the
534 experiments and that there may well be dose-dependent responses. Nevertheless they act as
535 a reasonable starting point for understanding the role of bacteria on ameliorating metal
536 toxicity to plants.

Acknowledgements

The authors are grateful for the financial support of the Rivers-State Sustainable Development Agency, Nigeria, and Diamond Light Source, Oxford U.K., for providing synchrotron beamtime through grant SP9151. The support of staff in the laboratories and glasshouses at the University of Edinburgh is also acknowledged.

Supporting Information. Characterization of experimental soil (S1). Details of experimental design, execution and analysis (S2-S4). Nanoparticles characterization (S5). Zinc concentrations in plant tissues (S6). XANES Linear Combination Fit (LCF) graphs (S7).

References

1. Morel, F. M. M.; Hering, J. G. *Principles and Applications of Aquatic Chemistry*; John Wiley & Sons Inc.: Somerset, New Jersey, 1993; pp 405-414.

2. Di Toro, D. M.; Allen, H. E.; Bergman, H. L.; Meyer, J. S.; Paquin, P.; Santone, R. C. Biotic ligand model of the acute toxicity of metals. 1. Technical basis. *Environ. Toxicol. Chem*. **2001**, 20, 2383-2396.

3. Khan, F. R.; Paul, K. B.; Dybowska, A. D.; Valsami-Jones, E.; Lead, J. R.; Stone, V.; Fernandes, T. F. Accumulation dynamics and acute toxicity of silver nanoparticles to *Daphnia magna* and *Lumbriculus variegatus*: implications for metal modeling approaches. *Environ. Sci .Technol*. **2015**, 49, 4389-4397.

4. López-Chuken, U. J.; Young, S. D.; Guzman-Mar, J. L. Evaluating a 'biotic ligand model' applied to chloride-enhanced Cd uptake by *Brassica juncea* from nutrient solution at constant Cd^{2+} activity. *Environ. Technol*. **2010**, 31, 307-318.

5. Bradfield, S. J.; Kumar, P.; White, J. C.; Ebbs, S. D. Zinc, copper, or cerium accumulation from metal oxide nanoparticles or ions in sweet potato: Yield effects and projected dietary intake from consumption. *Plant Physiol. Biochem*. **2017**, 110, 128-137.

6. Ma, L.; Wang, L.; Jia, Y.; Yang, Z. Arsenic speciation in locally grown rice grains from Hunan Province, China: Spatial distribution and potential health risk. *Sci. Total Environ*. **2016**, 557, 438-444.

7. Lin, D.; Xing, B. Root uptake and phytotoxicity of ZnO nanoparticles. *Environ. Sci. Technol.* **2008**, 42, 5580-5585.

8. Lv, J.; Zhang, S.; Luo, L.; Zhang, J.; Yang, K.; Christie, P. Accumulation, speciation and uptake pathway of ZnO nanoparticles in maize. *Environ. Sci. Nano*. **2015**, 2, 68-77.

9. López-Moreno, M.; de La Rosa, G.; Hernández-Viezcas, J. Á.; Castillo-Michel, H.; Botez, C.; Peralta-Videa, J.; Gardea-Torresdey, J. Evidence of the differential biotransformation and genotoxicity of ZnO and CeO_2 nanoparticles on soybean (*Glycine max*) plants. *Environ. Sci. Technol*. **2010**, 44, 7315-7320.

10. Hernandez-Viezcas, J. A.; Castillo-Michel, H.; Andrews, J. C.; Cotte, M.; Rico, C.; Peralta-Videa, J. R.; Ge, Y.; Priester, J. H.; Holden, P. A.; Gardea-Torresdey, J. L. In situ synchrotron X-ray fluorescence mapping and speciation of CeO_2 and ZnO nanoparticles in soil cultivated soybean (*Glycine max*). ACS Nano **2013**, 7, 1415.

11. Cruz, T. N. M.; Savassa, S. M.; Gomes, M. H. F.; Rodrigues, E. S.; Duran, N. M.; Almeida, E.; Martinelli, A. P.; Carvalho, H. W. P. Shedding light on the mechanisms of absorption and transport of ZnO nanoparticles by plants via in vivo X-ray spectroscopy. *Environ. Sci. Nano*. **2017**, 4, 2367-2376.

12. Hudson-Edwards, K. Tackling mine wastes. Science **2016**, 352, 288-290.

13. Isaure, M.P.; Laboudigue, A.; Manceau, A.; Sarret, G.; Tiffreau, C.; Trocellier, P.; Lamble, G.; Hazemann, J.L.; Chateigner, D. Quantitative Zn speciation in a contaminated dredged sediment by μ-PIXE, μ-SXRF, EXAFS spectroscopy and principal component analysis. *Geochim. Cosmochim. Acta* **2002**, 66, 1549-1567.

14. Liu, X.; Wang, F.; Shi, Z.; Tong, R.; Shi, X. Bioavailability of Zn in ZnO nanoparticle-spiked soil and the implications to maize plants. *J. Nanopart. Res*. **2015**, 17, 1-11.

15. Rao, S.; Shekhawat, G. S. Toxicity of ZnO engineered nanoparticles and evaluation of their effect on growth, metabolism and tissue specific accumulation in *Brassica juncea*. *J. Environ. Chem. Eng.* **2014**, 2, 105-114.

16. Gardea-Torresdey, J. L.; Rico, C. M.; White, J. C. Trophic transfer, transformation and impact of engineered nanomaterials in terrestrial environments. *Environ. Sci. Technol*. **2014**, 48, 2526-2540.

17. Du, W.; Tan, W.; Peralta-Videa, J. R.; Gardea-Torresdey, J. L.; Ji, R.; Yin, Y.; Guo, H. Interaction of metal oxide nanoparticles with higher terrestrial plants: Physiological and biochemical aspects. *Plant Physiol. Biochem.* **2017**, 110, 210–225.

18. Deng, R.; Lin, D.; Zhu, L.; Majumdar, S.; White, J.C.; Gardea-Torresdey, J. L.; Xing, B. Nanoparticle interactions with co-existing contaminants: joint toxicity, bioaccumulation and risk, *Nanotoxicology* **2017**, 11, 591-612.

19. Cakmak, I.; McLaughlin, M. J.; White, P. Zinc for better crop production and human health. *Plant Soil* **2017**, 411, 1-4.

20. Broadley, M. R.; White P. J.; Hammond, J. P.; Zelko, I.; Lux, A. Zinc in plants. *New Phytol.* **2007**, 173, 677-702.

21. Rascio, N.; Navari-Izzo, F. Heavy metal hyperaccumulating plants: How and why do they do it? And what makes them so interesting? *Plant Sci.* **2011**, 180, 169-181.

22. Salt, D. E.; Smith, R. D.; Raskin, I. Phytoremediation. *Annu. Rev. Plant Physiol. and Plant Mol. Biol.* **1998**, 49, 643-668.

23. Adediran, G. A.; Ngwenya, B. T.; Mosselmans, J. F. W.; Heal, K. V.; Harvie, B. A. Mechanisms behind bacteria induced plant growth promotion and Zn accumulation in *Brassica juncea*. *J. Hazard. Mater.* **2015**, 283, 490-499.

24 Rodríguez B. J.; Roca, N.; Febrero, A.; Bort, J. Assessment of heavy metal tolerance in two plant species growing in experimental disturbed polluted urban soil. *J. Soils Sediments* **2017**, 1-13.

25. Haney, H. C.; Samuel, B. S.; Bush, J.; Ausubel, F. M. Associations with rhizosphere bacteria can confer an adaptive advantage to plants. *Nat. Plants* **2015**, 1, No. 15051.

26. Pérez-de-Luque, A.; Tille, S.; Johnson, I.; Pascual-Pardo, D.; Ton, J.; Cameron, D. D. The interactive effects of arbuscular mycorrhiza and plant growth-promoting rhizobacteria synergistically enhance host plant defences against pathogens. *Sci. Rep.* **2017**, 7, No. 16409.

27. Benizri, E.; Kidd, P. S. The role of the rhizosphere and microbes associated with hyperaccumulator plants in metal accumulation. In *Agromining: Farming for Metals*; van der Ent, A., Echevarria, G., Baker, A. J. M., Morel, J. L., Eds.; Mineral Resource Reviews; Springer: Cham, Switzerland, 2018; pp 157-188.

28. Zhuang, X.; Chen, J.; Shim, H.; Bai, Z. New advances in plant growth-promoting rhizobacteria for bioremediation. *Environ. Int*. **2007**, 33, 406-413.

29. Dimkpa, C. O.; Merten, D.; Svatoš, A.; Büchel, G.; Kothe, E. Siderophores mediate reduced and increased uptake of cadmium by *Streptomyces tendae* F4 and sunflower (*Helianthus annuus*), respectively. *J. Appl. Microbiol*. **2009**, 107, 1687-1696.

30. Abou-Shanab, R.; Ghanem, K.; Ghanem, N.; Al-Kolaibe, A. The role of bacteria on heavy- metal extraction and uptake by plants growing on multi-metal-contaminated soils. *World J. Microbiol. Biotechnol*. **2008**, 24, 253-262.

31. Ganguly, S.; Das, S.; Dastidar, S. G. Study of antimicrobial effects of the anticancer drug oxaliplatin and its interaction with synthesized ZnS nanoparticles. *Int. J. Pharm. Therap.* **2014**, 5, 230-234.

32. Hammond, C. *The Basics of Crystallography and Diffraction*, 3rd ed.; Oxford University Press: Oxford, 2009.

33. Chami, Z.; Cavoski, I.; Mondelli, D.; Miano, T. Effect of compost and manure amendments on zinc soil speciation, plant content, and translocation in an artificially contaminated soil. *Environ. Sci. Pollut. Res*. **2013**, 20, 4766-4776.

34. Ebbs, S. D.; Kochian, L. V. Toxicity of zinc and copper to Brassica species: implication for phytoremediation. *J. Environ. Qual.* **1997**, 26, 776-781.

35. Zhao, L.; Yuan, L.; Wang, Z.; Lei, T.; Yin, X. Phytoremediation of zinc-contaminated soil and zinc-biofortification for human nutrition. In *Phytoremediation and Biofortification*. Yin, X., Yuan, L., Eds Springer Briefs in Molecular Science; Springer: Dordrecht, 2012; pp 33-57.

36. Allen; S. E.; Grimshaw, H. M.; Parkinson, J. A.; Quarmby, C. L. *Chemical Analysis of Ecological Materials.* Blackwell: Oxford, 1974.

37. Mosselmans, J. F. W.; Quinn, P. D.; Dent, A. J.; Cavill, S. A.; Moreno, S. D.; Peach, A.; Leicester, P. J.; Keylock, S. J.; Gregory, S. R.; Atkinson, K. D.; Rosell, J. R. I18 – the microfocus spectroscopy beamline at the Diamond Light Source. *J. Synchrotron Rad*. **2009**, 16, 818-824.

38. Solé, V. A.; Papillon, E.; Cotte, M.; Walter, P.; Susini, J. A multiplatform code for the analysis of energy-dispersive X-ray fluorescence spectra. *Spectrochim. Acta Part B: Atomic Spect*. **2007**, 62, 63-68.

39. Ravel, B.; Newville, M. Athena, Artemis, Hephaestus: data analysis for X-ray absorption spectroscopy using IFEFFIT. *J. Synchrotron Rad*. **2005**, 12, 535-541.

40. Whiting, S.; Leake, J.; McGrath, S.; Baker, A. Zinc accumulation by *Thlaspi caerulescens* from soils with different Zn availability: a pot study. *Plant Soil* **2001**, 236, 11-18.

41. Wang, P.; Menzies, N. W.; Lombi, E.; McKenna, B. A.; Johannessen, B.; Glover, C. J.; Kappen, P.; Kopittke, P. M. Fate of ZnO nanoparticles in soils and cowpea (*Vigna unguiculata*). *Environ. Sci. Technol*. **2013**, 47, 13822-13830.

42. Voegelin, A.; Jacquat, O.; Pfister, S.; Barmettler, K.; Scheinost, A. C.; Kretzschmar, R. Time dependent changes of zinc speciation in four soils contaminated with zincite or sphalerite. *Environ. Sci. Technol*. **2011**, 45, 255-261.

43. Franklin, N. M; Rogers, N. J., Apte, S. C.; Batley, G. E.; Gadd, G. E.; Casey, P.S. Comparative toxicity of nanoparticulate ZnO, bulk ZnO, and $ZnCl_2$ to a freshwater microalga (*Pseudokirchneriella subcapitata*): The importance of particle solubility. *Environ. Sci. Technol*. **2007**, 41, 8484–8490.

44. Mudunkotuwa, I. A.; Rupasinghe, T.; Wu, C. M.; Grassian, V. H.; Dissolution of ZnO nanoparticles at circumneutral pH: a study of size effects in the presence and absence of citric acid. Langmuir **2012**, 28, 396-403.

45. Eskelsen, J. R.; Xu, J.; Chiu, M.; Moon, J.; Wilkins, B.; Graham, D. E.; Gu, B., Pierce, E. M. Influence of structural defects on biomineralized ZnS nanoparticle dissolution: an in-situ electron microscopy study. *Environ. Sci. Technol* **2017**, DOI 10.1021/acs.est.7b04343.

699 46. Hafeez; B.; Khanif, Y. M.; Saleem, M. Role of zinc in plant nutrition - A review. *Am. J.*
700 *Exper. Agric.* **2013**, 3, 374-391.

701 47. Grewal, H.; Graham, R. Seed zinc content influences early vegetative growth and zinc
702 uptake in oilseed rape (*Brassica napus* and *Brassica juncea*) genotypes on zinc-deficient soil.
703 *Plant Soil.* **1997**, 192, 191-197.

704 48. Singh, S.; Sinha, S. Morphoanatomical response of two varieties of *Brassica juncea* (L.)
705 Czern. grown on tannery sludge amended soil. *Bull. Environ. Contam. Toxicol*. **2004**, 72, 1017-
706 1024.

707 49. Priester, J. H.; Ge, Y.; Mielke, R. E.; Horst, A. M.; Moritz, S. C.; Espinosa, K.; Gelb, J.;
708 Walker, S. L.; Nisbet, R. M.; An, Y.-J.; Schimel, J. P.; Palmer, R. G.; Hernandez-Viezcas, J. A.;
709 Zhao, L.; Gardea-Torresdey, J. L.; Holden, P. A. Soybean susceptibility to manufactured
710 nanomaterials with evidence for food quality and soil fertility interruption. *Proc. Natl. Acad.*
711 *Sci.* **2012**, 109, 14734-14735.

712 50. Dede, G., Ozdemir S. Effects of elemental sulphur on heavy metal uptake by plants
713 growing on municipal sewage sludge. *J. Environ. Manage.* **2016**, 166, 103-108.

714 51. Carciochi, W. D.; Divito, G. A.; Fernández, L. A.; Echeverría, H. E. Sulfur affects root
715 growth and improves nitrogen recovery and internal efficiency in wheat. *J. Plant Nutr*. **2017**,
716 40, 1231-1242.

717 52. Das, J.; Sarkar P. Remediation of arsenic in mung bean (*Vigna radiata*) with growth
718 enhancement by unique arsenic-resistant bacterium *Acinetobacter lwoffii*. *Sci. Total Environ.*
719 **2018**, 624, 1106-1118.

720 53. Khan, M.; Zaidi, A.; Wani, P.; Oves, M. Role of plant growth promoting rhizobacteria in
721 the remediation of metal contaminated soils. Environ. Chem. Lett. **2009**, 7, 1-19.

722 54. Ma, Y.; Oliveira, R. S.; Wu, L.; Luo, Y.; Rajkumar, M.; Rocha, I.; Freitas, H. Inoculation
723 with metal- mobilizing plant- growth- promoting Rhizobacterium *Bacillus* sp. SC2b and its role
724 in rhizoremediation. *J. Toxicol. Environ. Health, Part A* **2015a**, 78, 931-944.

725 55. Ma, Y.; Rajkumar, M.; Rocha, I.; Oliveira, R. S.; Freitas, H. Serpentine bacteria influence
726 metal translocation and bioconcentration of *Brassica juncea* and *Ricinus communis* grown in
727 multi-metal polluted soils. *Front. Plant Sci.* **2015b**, 5.

728 56. Ahmad, A.; Ghufran, R.; Zularisam, A. Phytosequestration of metals in selected plants
729 growing on a contaminated Okhla Industrial Areas, Okhla, New Delhi, India. *Water Air Soil*
730 *Pollut*. **2011**, 217, 255-266.

731 57. Marchiol, L.; Assolari, S.; Sacco, P.; Zerbi, G. Phytoextraction of heavy metals by canola
732 (*Brassica napus*) and radish (*Raphanus sativus*) grown on multi contaminated soil. *Environ.*
733 *Pollut*. **2004**, 132, 21-27.

734 58. Brunetti, G.; Soler-Rovira, P.; Farrag, K.; Senesi, N. Tolerance and accumulation of
735 heavy metals by wild plant species grown in contaminated soils in Apulia region, Southern
736 Italy. *Plant Soil* **2009**, 318, 285-298.

737 59. Zhang, Y. F.; He, L. Y.; Chen, Z. J.; Wang, Q. Y.; Qian, M.; Sheng, X. F. Characterization
738 of ACC deaminase-producing endophytic bacteria isolated from copper-tolerant plants and
739 their potential in promoting the growth and copper accumulation of *Brassica napus.*
740 *Chemosphere* **2011**, 83, 57-62.

741 60. Zhang, Y. F.; He, L. Y.; Chen, Z. J.; Zhang, W. H.; Wang, Q. Y.; Qian, M.; Sheng, X. F.
742 Characterization of lead-resistant and ACC deaminase-producing endophytic bacteria and
743 their potential in promoting lead accumulation of rape. *J. Hazard. Mater*. **2011,** 186, 1720-
744 1725.

745 61. Rajkumar, M.; Ma, Y.; Freitas, H. Improvement of Ni phytostabilization by inoculation
746 of Ni resistant *Bacillus megate*rium SR28C. *J. Environ. Manag*. **2013**, 128, 973-980.

747 62. Zhang, D.; Hua, T.; Xiao, F.; Chen, C.; Gersberg, R. M.; Liu, Y.; Stuckey, D.; Ng, W. J.;
748 Tan. S. K. Phytotoxicity and bioaccumulation of ZnO nanoparticles in *Schoenoplectus*
749 *tabernaemontani*. *Chemosphere* **2015**, 120, 211-219.

750 63. Kopittke, P. M.; Menzies, N. W.; de Jonge, M. D.; McKenna, B. A.; Donner, E.; Webb,
751 R. I.; Paterson, D. J.; Howard, D. I.; Ryan, C. G.; Glover, C. J.; Scheckel, K. G.; Lombi, E. In situ
752 distribution and speciation of toxic copper, nickel, and zinc in hydrated roots of cowpea. *Plant*
753 *Physiol.* **2011**, 156, 663-673.

754 64. Sarret, G.; Saumitou-Laprade, P.; Bert, V.; Proux, O.; Hazemann, J. L.; Traverse, A.;
755 Marcus, M. A.; Manceau, A. Forms of zinc accumulated in the hyperaccumulator *Arabidopsis*
756 *halleri*. *Plant Physiol*. **2002**, 130, 1815-1826.

757 65. Terzano, R.; Chami, Z. A.; Vekemans, B.; Janssens, K.; Miano, T.; Ruggiero, P. Zinc
758 distribution and speciation within rocket plant (*Eruca vesicaria* L. *Cavalieri*) grown on a
759 polluted soil amended with compost as determined by XRF microtomography and micro-
760 XANES. *Agric. Food Chem.* **2008**, 56, 3222-3231.

761 66. Adediran, G. A.; Ngwenya, B. T.; Mosselmans, J. F. W.; Heal, K.V. Bacteria–zinc co-
762 localization implicates enhanced synthesis of cysteine-rich peptides in zinc detoxification
763 when *Brassica juncea* is inoculated with *Rhizobium leguminosarum*. *New Phytol*. **2016a**, 209,
764 280-293.

765 67. Singh, V. P. *Metal Toxicity and Tolerance in Plants and Animals*. Sarup & Sons: New
766 Delhi, India, 2005; p 328.

767 68. Kühnlenz, T.; Hofmann, C; Uraguchi, S.; Schmidt, H.; Schempp, S.; Webber, M.; Brett,
768 L.; Salt, D. E.; Clemens, S. Phytochelatin synthesis promotes leaf Zn accumulation of
769 *Arabidopsis thaliana* plants grown in soil with adequate Zn supply and is essential for survival
770 on Zn-contaminated soil. *Plant Cell Physiol.* **2016**, 57, 2342–2352.

771 69. Krämer, U.; Cotter-Howells, J. D.; Charnock, J. M.; Baker, A. J. M.; Smith, J. A. C. Free
772 histidine as a metal chelator in plants that accumulates nickel. *Nature* **1996**, 379, 635-638.

773 70. Leitenmaier, B.; Küpper, H. Compartmentation and complexation of metals in
774 hyperaccumulator plants. *Front. Plant Sci*. **2013**, 4, No. 374.

775 71. Adediran, G. A.; Ngwenya, B. T.; Mosselmans, F. W.; Heal, K. V.; Harvie, B. A. Mixed
776 planting with a leguminous plant outperforms bacteria in promoting growth of a metal
777 remediating plant through histidine synthesis. *Int. J. Phytoremediat*. **2016b**, 18, 720-729.

778 72. Dimpka, C. O.; Latta, D. E.; McLean, J. E.; Britt, D. W.; Boyanov, M. I.; Anderson, A. J.
779 Fate of CuO and ZnO nanoparticles in the plant environment. *Environ. Sci. Technol*. **2013**, 47,
780 4734-4742.

781 73. Ma, X.; Geiser-Lee, J.; Deng, Y.; Kolmakov, A. Interactions between engineered
782 nanoparticles (ENPs) and plants: Phytotoxicity, uptake and accumulation. *Sci. Total Environ*.
783 **2010**, 408, 3053-3061.

Supporting Information

Soil bacteria override speciation effects on zinc phytotoxicity in zinc-contaminated soils

Nyekachi C. Adele[a*], Bryne T. Ngwenya[a], Kate V. Heal[a], and J. Frederick W. Mosselmans[b]

[a]School of GeoSciences, University of Edinburgh, Edinburgh, UK; [b]Diamond Light Source, Harwell Science and Innovation Campus, Didcot, UK

*Corresponding author contact details:

School of GeoSciences, University of Edinburgh, Grant Institute, James Hutton Road, The King's Buildings, Edinburgh EH9 3FE, UK

Email: kachia6@yahoo.com

Number of pages: 11

Number of figures: 5

Number of tables: 1

S1: Characterization of soil

Table S1. Physical and chemical properties of the experimental soil. Values are means of the analysis of air-dried, sieved (<2 mm) sub-samples (n shown in parentheses).

Parameters	Mean value (number of sub-samples)
Moisture content (%)	26.2 (3)
Organic matter content (% loss on ignition at 450°C)	15.4 (6)
pH (soil: deionized water m:v (1:2))	6.2 (1)
N (mg g^{-1})	1.79 (4)
P (mg g^{-1})	0.31 (4)
K (mg g^{-1})	8.49 (4)
Zn (mg g^{-1})	0.025 (4)
S (mg kg^{-1})	249 (2)

S2: Pot experiments

In the primary experiment, conducted in July-August 2014, plant growth and metal content of soil and plant materials were measured. A second experiment was conducted in December 2014-February 2015 to provide fresh material for synchrotron based X-ray spectroscopic analysis. The experiments were conducted in a greenhouse at the School of Biological Sciences, University of Edinburgh, set to provide a day/night temperature of 21°C in a 18 h photoperiod at a photosynthetic photon flux density (PPFD) of 150 µmol m^{-2} s^{-1} provided by cool white fluorescent bulbs.

Both experiments were set-up in exactly the same manner. The soil was air dried, crushed and passed through a 2 mm stainless steel sieve, and then mixed with 10% sand by volume to aid drainage. Next the soil was sterilized (134°C for 4 min in a BMM Weston autoclave) and amended with 600 mg Zn kg^{-1} in the form of $ZnSO_4$, ZnS and ZnO nanoparticles. The soil was spiked in 9 kg batches with different Zn species, and each batch mixed by hand for 1 h to distribute Zn contamination evenly. Plant growth experiments contained 12 treatments (including controls), with each replicated in three pots. Each 2.15 L pot contained 1 kg of spiked ($ZnSO_4$, ZnO and ZnS) or un-spiked soil (control). Both spiked and control pots were watered with deionized water and placed in individual trays throughout the experiment. The locations of the pots were randomized by assigning a number to each pot and using a manual technique to select pots at random in the greenhouse space. Soils were left to equilibrate for a week in the greenhouse before planting, following a similar time frame to previous studies,[1] which for the soil type would allow interaction with soil minerals while also maximizing bioavailability toxicity to plants. Although the experimental soil was sterilized initially, the greenhouse was not a sterile environment.

For bacterial inoculation, *Rhizobium legumniosarum* bv. *trifolii* and *Pseudomonas brassicacearum* were selected for their tolerance to Zn and their demonstrated ability to promote growth of *Brassica juncea*.[1-2] *R. leguminosarum* bv. *trifolii* (strain WSM1325) was isolated from the rhizosphere of a clover plant (School of Biological Sciences, University of Edinburgh, UK). *P. brassicacearum* subsp. *brassicacearum* (strain DBK11) was, obtained as a lyophilizate from the German collection of microorganisms and cell cultures (Leibniz Institute, DSMZ Germany; DSM number 13227). The bacteria strains (*R. leguminosarum* and *P. brassicacearum*) were grown in a nutrient medium (containing 1 g meat extract, 2 g yeast extract, 5 g peptone, 5 g NaCl, pH 7.4) for 2 days before being harvested, centrifuged, and washed three times with sterile deionized water. The pelleted cells were re-suspended in sterile deionized water to 10^8 CFU mL^{-1}.

Prior to inoculation, seeds of *B. juncea* were surface sterilized with 5% NaClO for 15 min and washed three times with sterile deionized water under a laminar flow hood. Seeds were soaked for 4 h in 10 mL bacteria suspension and uninoculated seeds were soaked in sterilized deionized water over the same duration before sowing 5 seeds in each pot. Seedlings were thinned out to 3 plants per pot at 12 days after planting. Pots were individually irrigated with tap water from the tray twice a week throughout the experiments.

S3: Plant sampling, and bioaccumulation analysis

All plants were harvested 6 weeks after planting of seeds. Shoots were cut 2 cm above the soil surface and washed with running tap water. Pots were emptied and roots were separated and washed in tap water to remove soil particles from the root surface. The harvested plant material (roots and shoots separately) was oven dried to constant weight at 65°C for 72 h and then weighed to determine biomass. Dried samples were finely ground using mortar and pestle and stored in polyethylene tubes prior to acid digestion for analysis. Total Zn concentrations in duplicate sub-samples of the ground plant materials and soil (batched for each treatment from the 3 replicate pots) were determined as described by Allen et al.[3] 6 mL concentrated HCl and 1 mL HNO_3 were used for digestion of 0.5 g ashed soil samples and 2 mL concentrated H_2SO_4 and 0.75 mL H_2O_2 (30%) were used for digestion of 0.1 g plant material samples. Zn concentrations were determined in the digest by inductively coupled plasma-optical emission spectrometry (ICP-OES) (Perkin Elmer Optima 5300 DV), with calibration standards made from Zn stock standard solution. The calibration standards required an R^2 value of at least 0.9999 in order to present a satisfactory calibration curve. Quality control blank checks and external calibration verification checks were run regularly throughout the analysis. An external standard (Merck ICP Multi element standard solution VI CertiPUR®) was analyzed at different dilutions as a cross reference for the calibration graphs. Zn concentrations measured in digest blanks were subtracted from the sample results.

The total Zn concentrations from soil and plant analysis were used to evaluate Zn phytoextraction by *Brassica juncea* (L.) Czern. The mean of the duplicate subsamples of each material was calculated to provide the single Zn concentration data used in the bioaccumulation factors, translocation factors and phytoextraction efficiency for each treatment combination.

The bioaccumulation factor (BCF) is the ratio of the concentration of metal in the plant tissue to the initial metal concentration in the soil.[4] The Translocation factor (TF) is the ratio of the metal concentration of the plant shoot to the metal concentration of the root.[4] Phytoextraction efficiency (PE) is the ratio of the mass of an element in the plant shoot to that in soil, expressed as a %,

$$PE(\%) = \frac{Mshoot \times Wshoot}{Msoil \times Wsoil} \times 100 \quad \text{(Equation 1)}$$

where M_{shoot} is the metal concentration in shoots of the plants (mg kg^{-1}), W_{shoot} is the dry plant above ground biomass (g), M_{soil} is the initial metal concentration in soil (mg kg^{-1}) and W_{soil} is the mass of soil in the pot (g). PE values reflect the amount of remediation of a metal by plant shoots from soil.[5]

S4: Synchrotron based X-ray spectroscopic analysis

The second pot experiment in 2014-15 was conducted using an identical procedure to provide live plant material for Zn speciation analysis by X-ray absorption. Live plants were used to avoid sample treatments such as freezing and, drying that could alter Zn speciation. Live plants were transported for harvest and micro X-ray fluorescence (µXRF) and micro X-ray absorption near edge structure (µXANES) analyses at beamline I18 at Diamond Light Source, UK. At harvest, live roots and shoots of *Brassica juncea* grown in soil amended with 600 mg kg^{-1} of different Zn species were washed thoroughly with deionized water to eliminate any surface contaminants. Root and shoot samples were cut with a scalpel, embedded in Meta-mix for 8 h and then axially sectioned (30 µm thickness) using a Reichert Ultracut microtome. The sample section was placed on a sapphire disc, covered with Kapton® tape and loaded into an Al sample holder, in a nitrogen cryostat, with the sample inclined at an angle of 45^{o} to the incident beam. Zinc distribution in root and shoot samples was mapped with an incident energy of 10.5 keV. XRF mapping was performed on areas of 0.5 x 0.5 mm with 2 µm resolution. From the mapping regions of high Zn concentration were identified for the collection of µXANES data at the Zn K-edge. X-ray absorption spectra were collected in fluorescence mode using a nine- element ORTEC germanium solid state detector placed in the horizontal plane at a right angle to the beam axis to reduce detection of elastically scattered photons. The energy was scanned through the absorption edge of Zn (9630-9850 eV). Ca. 5 scans of 20 min each were recorded and averaged at each spot analyzed. These high Zn regions were selected for collection of µXANES spectra. Due to the long time required to analyze each sample, data collection focused more on the inoculated (*Pseudomonas brassicacearum*) and uninoculated root samples.

Zn K-edge µXANES spectra were also collected under similar beam conditions for selected Zn standards (ZnS nanoparticles, Zn oxalate, Zn phosphate, Zn histidine, Zn cysteine, Zn phytate, Zn formate, Zn polygalacturonate, ZnO nanoparticles, preparation detailed in Adediran et al., 2016).[6] Specifically, nanoparticles were prepared as pellets diluted in cellulose whereas all the others standards were made in solutions of 70 mM Zn-ligand complexes. The monochromator was calibrated using a Zn foil scan (edge position 9659 eV). Zn solid standards were made into pellets using cellulose, whereas liquid forms were loaded on Al cells covered with Kapton® tape. The XRF spectra were analyzed using PyMCA 4.4.1 software.[7] In order to assess chemical species information, all µXANES spectra collected from the samples and standards were normalized and aligned. Linear Combination Fitting (LCF) was used through the Athena IFFEFIT software package[8] to identify the relative proportions of Zn reference spectra within the samples. The goodness of the fit was estimated by determining the residual R factor between the root sample and the Zn standard fits,

$$R = \frac{\sum(\text{data} - \text{fit})^2}{\sum(\text{data})^2} \qquad \text{(Equation 2)}$$

A lower R factor represents the best fit between the sample spectrum and the fitted standard spectra.[9] The spectra and their fits are shown in Figure S5.

S5: Nanoparticles Characterization

ZnS nanoparticles synthesized in our laboratory were characterized by powder X-Ray Diffraction (XRD) and by Transmission Electron Microscopy (TEM). Details are given in the main text and Figure S1 shows a representative XRD output and TEM images.

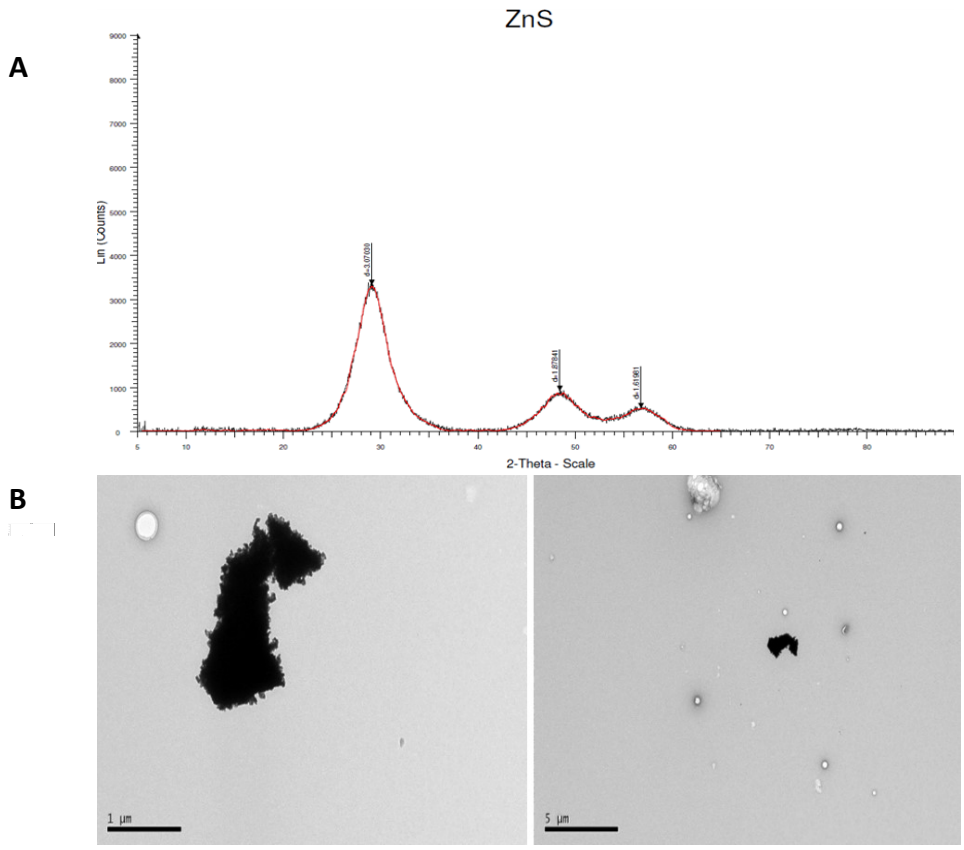

Figure S1: A XRD diffractogram of synthesized ZnS nanoparticles suggesting sphalerite structure and B transmission electron micrographs of synthesized ZnS nanoparticles showing aggregation.

The dissolution of ZnO and ZnS nanoparticles in water was measured over a 4-day experiment by suspending the nanoparticles in deionized water to a nominal concentration of 600 mg L^{-1} in elemental Zn, consistent with the Zn dose in the experimental soil. The starting pH of the suspensions was 6.2 and final pH was 5.77 (ZnO) and 5.79 (ZnS). Experiments were carried out in glass jars purged with oxygen-free nitrogen and sealed with butyl rubber-lined crimp seals. This approach was designed to limit oxidative dissolution of ZnS *via* sulfide oxidation so that we could compare the stoichiometric dissolution only. Although this might differ from the soil environment, we believe oxygen penetration in the soil treatments was likely limited by the pot watering regime to maintain soil moisture content (see section S2 above). Microcosms were set up in duplicate, and sampled once per day using a syringe followed by centrifugal filtration through a 3 kD pore filter for 30 min at 5,000 g. The filtrate was acidified to 2% in HNO acid and analyzed for dissolved Zn using ICP-OES as above (section S3). At the end of the experiment, a diluted suspension of each microcosm was analysed for particle size distribution using a Zetasizer (Nano ZS, Malvern, UK).

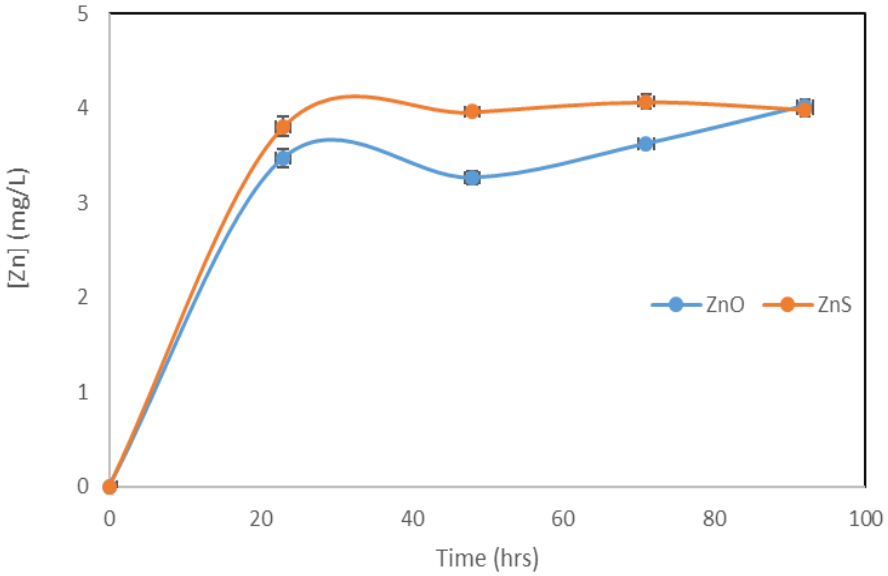

Figure S2: Concentration of Zn against time during dissolution of ZnO and ZnS nanoparticles in ultrapure water**.**

Time course Zn concentrations are slightly lower in ZnO suspensions, but the differences are small (~0.4 mg L^{-1}) and indeed concentrations are identical at the end of the experiment (92 h). During the experiment, we noted significant aggregation of the ZnO nanoparticles, forming aggregates in the mm size range. This is a feature reported by numerous previous studies (e.g.[10-11]), and was confirmed by particle size analysis, showing large sizes for ZnO compared to ZnS (Figure S3). Thus, all else being equal, it is likely that Zn concentrations in ZnO will be higher, especially as our measured Zn concentrations are comparable to those in previous studies (e.g.[11]) for similar nominal nanoparticle sizes.

		Size (d.nm):	% Intensity:	St Dev (d.nm):
Z-Average (d.nm): 1935	Peak 1:	2204	100.0	292.1
PdI: 0.236	Peak 2:	0.000	0.0	0.000
Intercept: 0.937	Peak 3:	0.000	0.0	0.000

Result quality : Refer to quality report

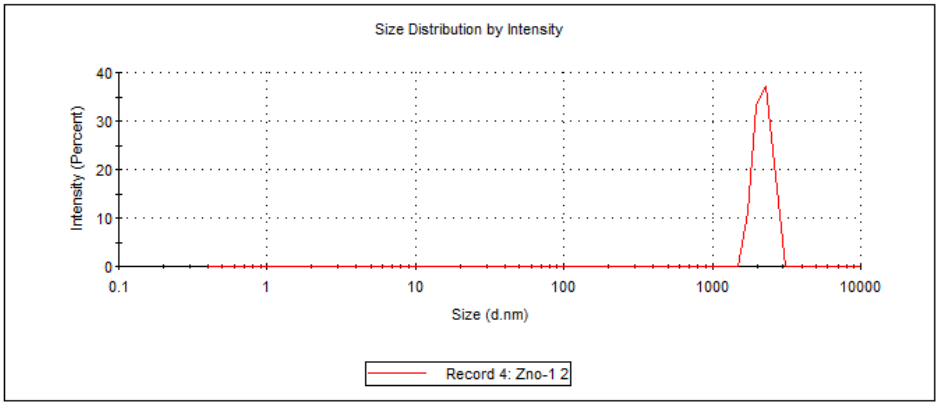

		Size (d.nm):	% Intensity:	St Dev (d.nm):
Z-Average (d.nm): 5653	Peak 1:	825.0	100.0	1.079e-5
PdI: 0.246	Peak 2:	0.000	0.0	0.000
Intercept: 0.996	Peak 3:	0.000	0.0	0.000

Result quality : Refer to quality report

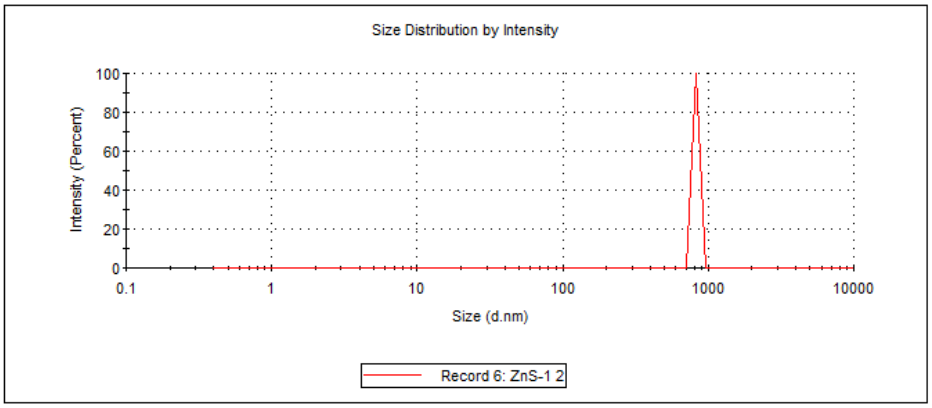

Figure S3. Particle size analysis of nanoparticle suspensions at the end of dissolution experiments. Note the larger average size for ZnO (2204 nm) compared to ZnS (825 nm).

S6: Zinc accumulation in plant tissues

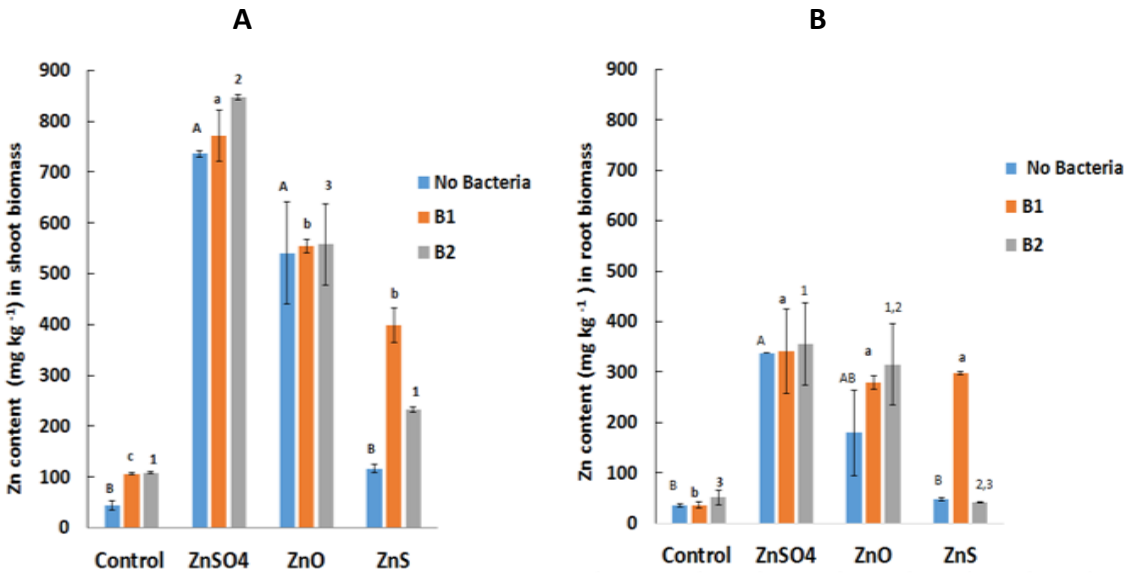

Figure S4: Zn concentrations in inoculated and uninoculated A shoot biomass and B root biomass 6 weeks after planting in Zn contaminated soil. Bars are means and error bars are standard error of mean of three pots. Different letters and symbols indicate significant ($p<0.05$) differences in Zn contents. B1 is *Rhizobium leguminosarum* and B2 is *Pseudomonas brassicacearum*.

S7: XANES Linear Combination Fit (LCF) graphs

Figure S5: Data were fitted over the range 9650-9710 eV

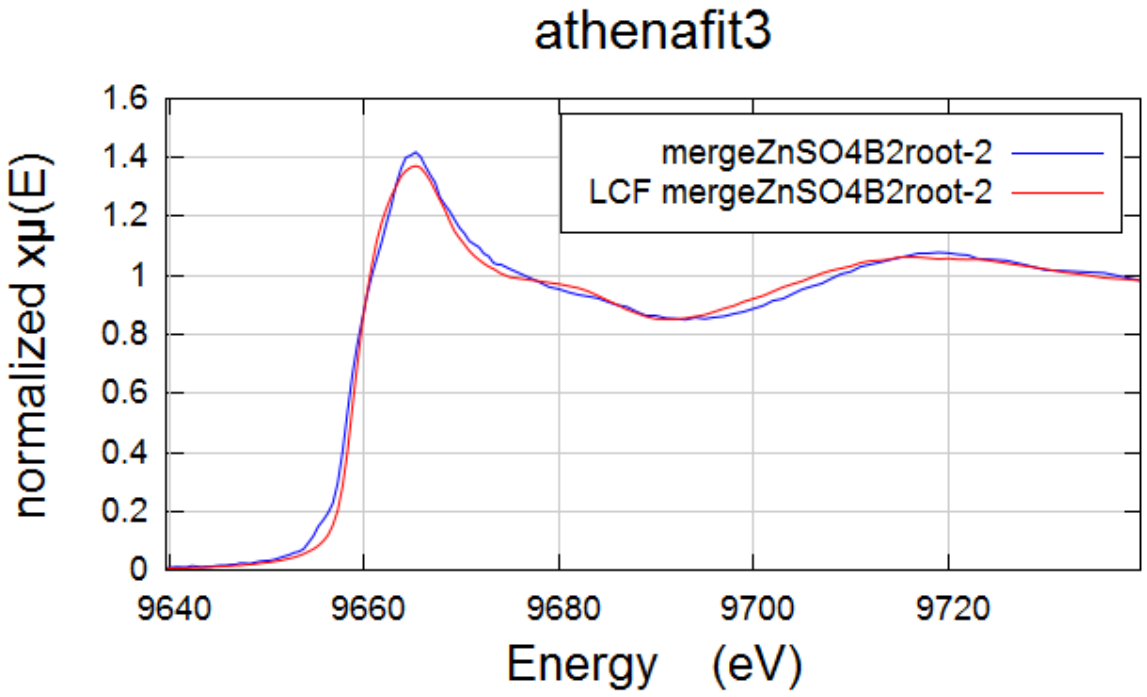

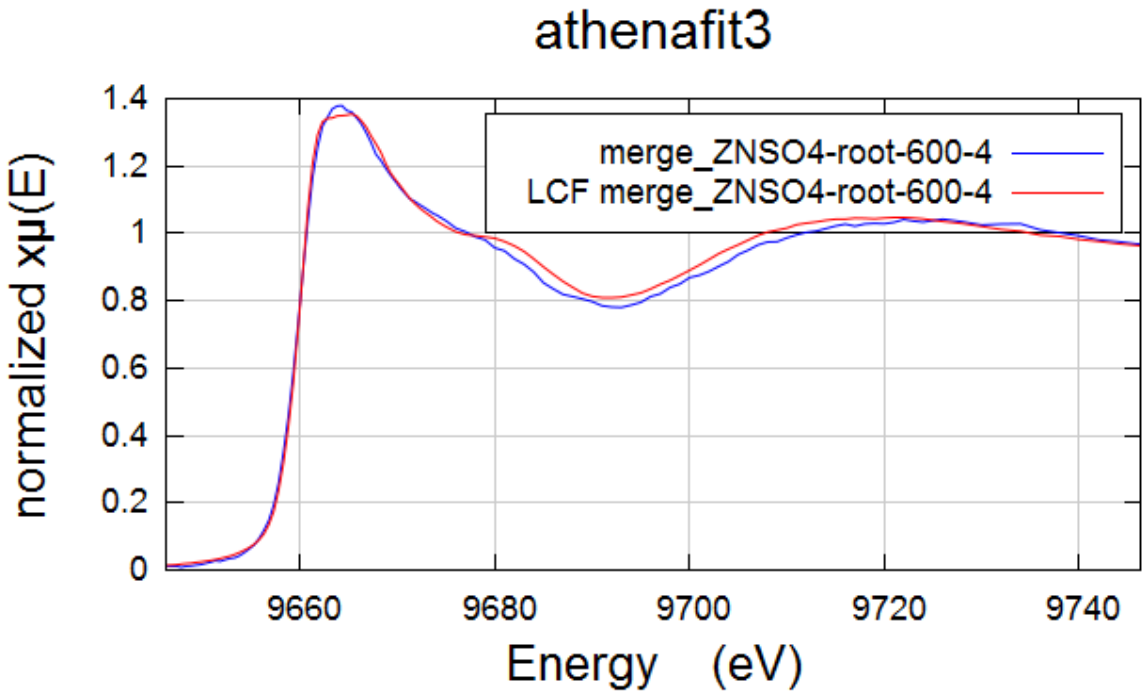

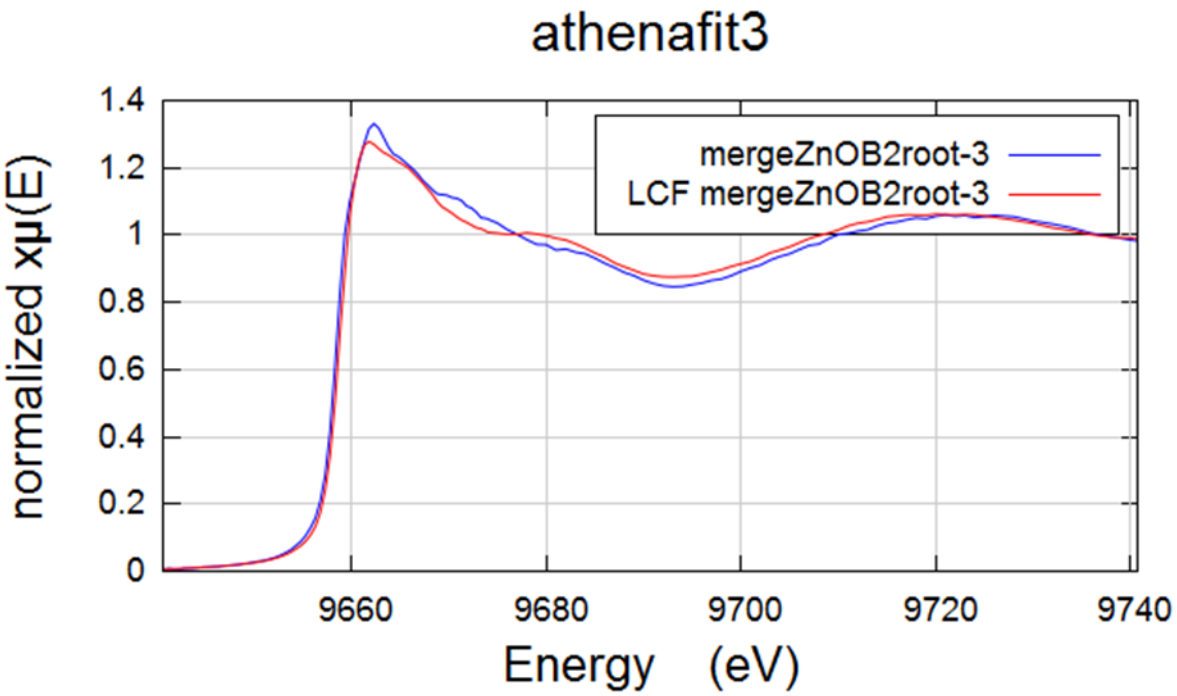

250

251

252

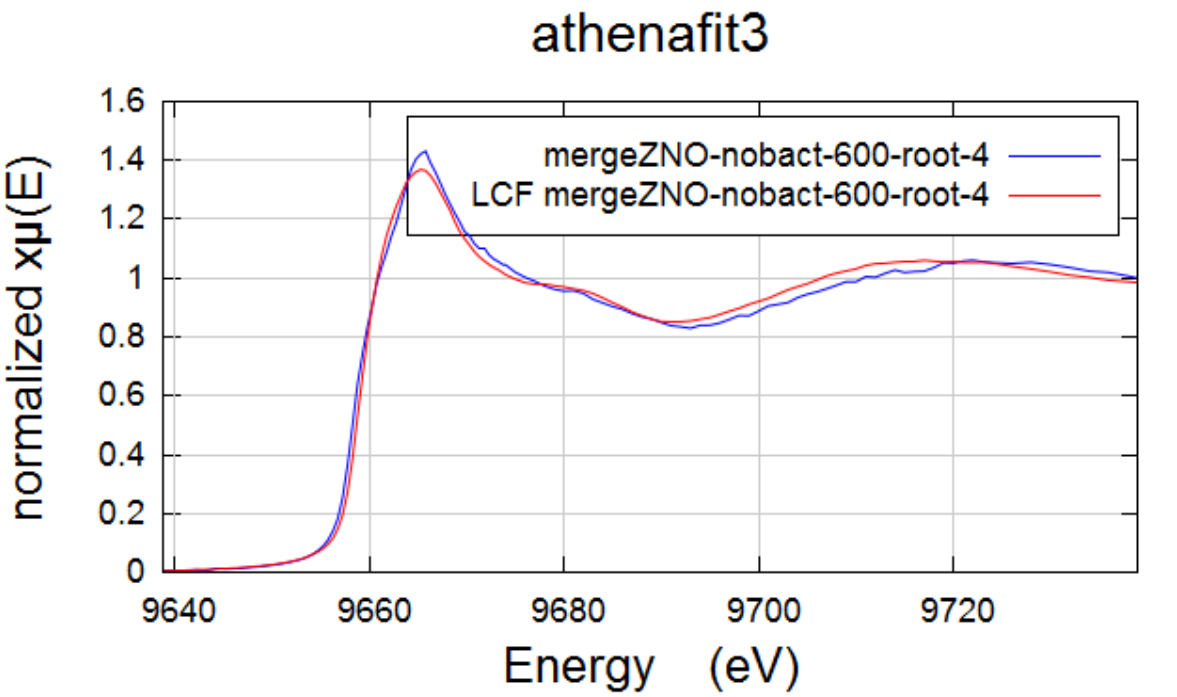

253

254

255

256

REFERENCES

1. Adediran, G. A.; Ngwenya, B. T.; Mosselmans, J. F. W.; Heal, K. V.; Harvie, B. A. Mechanisms behind bacteria induced plant growth promotion and Zn accumulation in *Brassica juncea*. *J. Hazard. Mater.* **2015**, 283, 490-499.

2. Zhuang, X.; Chen, J.; Shim, H.; Bai, Z. New advances in plant growth-promoting rhizobacteria for bioremediation. *Environ. Int*. **2007**, 33, 406-413.

3. Allen; S. E.; Grimshaw, H. M.; Parkinson, J. A.; Quarmby, C. L. *Chemical Analysis of Ecological Materials.* Blackwell: Oxford, 1974.

4. Ma, Y.; Rajkumar, M.; Rocha, I.; Oliveira, R. S.; Freitas, H. Serpentine bacteria influence metal translocation and bioconcentration of *Brassica juncea* and *Ricinus communis* grown in multi-metal polluted soils. *Front. Plant Sci.* **2015b**, 5.

5. Mani, D.; Kumar, C.; Patel, N. K. Integrated micro-biochemical approach for phytoremediation of cadmium and zinc contaminated soils. *Ecotoxicol. Environ. Saf*. **2015,** 111, 86-95.

6. Adediran, G. A.; Ngwenya, B. T.; Mosselmans, F. W.; Heal, K. V.; Harvie, B. A. Mixed planting with a leguminous plant outperforms bacteria in promoting growth of a metal remediating plant through histidine synthesis. *Int. J. Phytoremediat*. **2016b**, 18, 720-729.

7. Solé, V. A.; Papillon, E.; Cotte, M.; Walter, P.; Susini, J. A multiplatform code for the analysis of energy-dispersive X-ray fluorescence spectra. *Spectrochim. Acta Part B: Atomic Spect*. **2007**, 62, 63-68.

8. Ravel, B.; Newville, M. Athena, Artemis, Hephaestus: data analysis for X-ray absorption spectroscopy using IFEFFIT. *J. Synchrotron Rad*. **2005**, 12, 535-541.

9. Terzano, R.; Chami, Z. A.; Vekemans, B.; Janssens, K.; Miano, T.; Ruggiero, P. Zinc distribution and speciation within rocket plant (*Eruca vesicaria* L. *Cavalieri*) grown on a polluted soil amended with compost as determined by XRF microtomography and micro-XANES. *Agric. Food Chem.* **2008**, 56, 3222-3231.

10. Franklin, N. M; Rogers, N. J., Apte, S. C.; Batley, G. E.; Gadd, G. E.; Casey, P.S. Comparative toxicity of nanoparticulate ZnO, bulk ZnO, and $ZnCl_2$ to a freshwater microalga (*Pseudokirchneriella subcapitata*): The importance of particle solubility. *Environ. Sci. Technol*. **2007**, 41, 8484–8490.

11. Mudunkotuwa, I. A.; Rupasinghe, T.; Wu, C. M.; Grassian, V. H.; Dissolution of ZnO nanoparticles at circumneutral pH: a study of size effects in the presence and absence of citric acid. Langmuir **2012**, 28, 396-403.